

DT ①

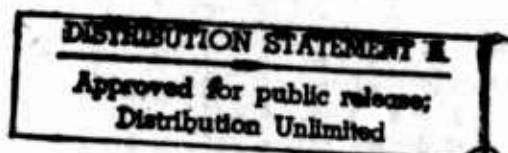
FORTIFIKATORISK

AD725157

NOTAT NR. 48 / 69

Reproduced by
NATIONAL TECHNICAL
INFORMATION SERVICE
Springfield, Va. 22151

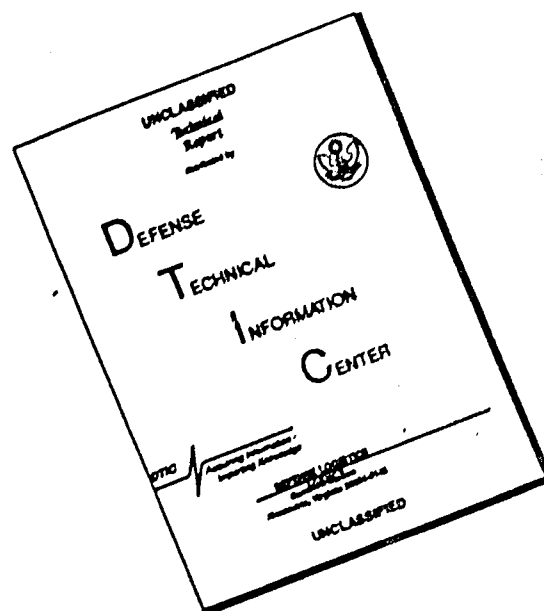
ONE-DIMENSIONAL BLAST WAVE PROPAGATION



FORSVARETS BYGNINGSTJENESTE

Incl # 4

DISCLAIMER NOTICE



THIS DOCUMENT IS BEST QUALITY AVAILABLE. THE COPY FURNISHED TO DTIC CONTAINED A SIGNIFICANT NUMBER OF PAGES WHICH DO NOT REPRODUCE LEGIBLY.

NORWEGIAN DEFENCE CONSTRUCTION SERVICE
Office of Test and Development

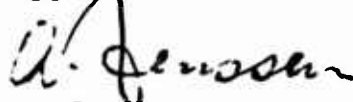
Fortifikatorisk notat nr N 48/69

ONE-DIMENSIONAL BLAST WAVE PROPAGATION

by

Arne Skjeltorp

Approved:



A. Jenssen
Chief Office of Test and Development

August 1968

Acknowledgements

This is a final test report of a series of preliminary experiments concerning the feasibility of model tests used for the prediction of one-dimensional blast wave propagation. The experiments were partly supported and encouraged by the following institutions:

Grubernes Sprængstofffabriker A/S
Nitro Nobel AB (Sweden)
Norsk Sprængstofindustri A/S
Raufoss ammunisjonsfabrikker
Sprengstoffinspeksjonen

We would especially point out the efforts made by Ø. Smeby, Raufoss ammunisjonsfabrikker and K. Wenstøp, Norsk Sprængstofindustri A/S in selecting test sites, supporting explosives etc.

We also appreciate the interest and critical reading of the manuscript by Dr T.A. Zaker, Armed Services Explosives Safety Board, Washington D.C. and Mr C.A. Coulter, Ballistic Research Laboratories, U.S. Army Aberdeen Research and Development Center.

Personnel responsible for the experiments, include:

E. Berg, K. Henriksen, A.Jenssen and A. Skjeltorp, Norwegian Defence Construction Service, Office og Test and Development.

ABSTRACT

This report is a summary of the results of a series of experiments on one-dimensional blast wave propagation in steeltubes, diameter 5 cm and 20 cm, in a concrete tube of diameter 80 cm and in a tunnel in rock of effective diameter 6 m. The blast waves originated from detonation of TNT charges placed in the center of the tubes/tunnel. Measurements of pressure time history, employing piezoelectric pressure transducers, show that frontpressure, impulse, positive duration and time of arrival scaled according to common one-dimensional scaling laws for small distances, L/D , expressed in diameter units, and for longer distances gave deviations with L/D more or less as parameter. The effects of varying wall roughness is not investigated in detail, but estimates of exponential damping constants are given.

TABLE OF CONTENTS

	Page
ABSTRACT	ii
I. INTRODUCTION	1
II. SCALING	2
II.1 Dimensional analysis	2
II.2 The principle of similarity in one-dimensional blast wave propagation	3
II.3 Attenuation in long tunnels	6
III. TEST PROGRAM	9
III.1 General	9
III.2 Roughness of tubes and tunnel in rock	11
III.3 Explosive charges	11
III.4 Transducers	12
III.5 Transducer mounting	14
III.6 Instrumentation	15
III.7 Check of frontpressure with time-of-flight measurements	19
IV. PREPARATION OF DATA	21
IV.1 Interpretation of traces	21
IV.2 Conversion of picture to paper-tape	21
IV.3 Computer work	22
V. RESULTS AND DISCUSSION	24
V.1 Frontpressure	24
V.2 Impulse	40
V.3 Positive duration	47
V.4 Time of arrival	49
VI. SUMMARY	51
References	54

LIST OF ILLUSTRATIONS

<u>Figure Number</u>		<u>Page</u>
II.1	Plane charges filling the whole tube cross section	4
II.2	Spherical charges in tubes	5
II.3	Blast wave formation inside a tube ..	7
II.4	Deviation from ideal scaling	7
II.5	80 cm diameter concrete tube at test site	10
II.6	5 cm diameter steel tube with trans- ducer mounting and arrangement for time-of-flight measurements	10
III.1	Definition of roughness $\frac{e}{D}$. 100%	11
III.2	Typical TNT-charges used	12
III.3	Dimensions of LC-33 transducer	13
III.4	Typical pressure-time profile	13
III.5	Transducer mounted in 5 and 20 cm tube	14
III.6	Transducer mounted in 80 cm tube ...	15
III.7	Transducer mounted in 6 m tunnel in rock	15
III.8	Schematic electrical flow chart for 5 and 20 cm diameter tube tests	16
III.9	Schematic electrical flow chart for 80 cm tube and 6 m diameter tunnel in rock tests	17
III.10	Typical records from oscilloscope and oscillograph	18
III.11	Comparison pressure-time measurements and velocity measurements in 5 cm tube	20
IV.1	Definition of parameters	21
IV.2	Schematic conversion of pictures to paper-tape	22
V.1	Frontpressure versus tube position in L/D units 5 cm tube	26
V.2	Frontpressure versus tube position in L/D units in 20 cm tube	27
V.3	Frontpressure versus tube position in L/D units in 80 cm tube	28

	Page
V.4 Frontpressure versus tunnel position in L/D units in 6 m tunnel in rock	29
V.5 Comparison of frontpressure attenua- tion for different tubes and tunnel in rock	30
V.6 "Attenuation" constant k_1 for longrange attenuation versus initial frontpressure p_{20} at L/D = 20 from figures V.1 to V.5	31
V.7 Functional dependance of $C(P_{20})$...	32
V.8 Frontpressure versus equivalent charge weight for 5 cm diameter tube	34
V.9 Frontpressure versus equivalent charge weight for 20 cm diameter tube	35
V.10 Frontpressure versus equivalent charge weight for 80 cm diameter tube	36
V.11 Frontpressure versus equivalent charge weight for 6 m diameter tunnel in rock	37
V.12 Averaged frontpressure curves versus equivalent charge weight	38
V.13 Fractional changes in pressure from scaled unattenuated curve per unit distance of travel in tube diameters	40
V.14 Reduced impulse versus equivalent charge weight for 5 cm and 20 cm diameter tube	42
V.15 Reduced impulse versus equivalent charge weight for 80 cm diameter tube.....	43
V.16 Reduced impulse versus equivalent charge weight for 6 m diameter tunnel in rock	44
V.17 Reduced impulse versus equivalent charge weight compared	45
V.18 Reduced impulse versus equivalent charge weight compared	46
V.19 Reduced positive duration versus equiva- lent charge weight	48
V.20 Reduced time of arrival versus equiva- lent charge weight	50
VI.1 Reduced "smooth wall" scaled blast wave data	53

LIST OF TABLES

<u>Table</u>	<u>Page</u>
III.1 Test Description	9
III.2 Nominal characteristics for LC-33 transducer	13

NOMENCLATURE

C	attenuation constant defined in text
D	major inside tube/tunnel diameter
e	averaged absolute wall roughness
$e/D \cdot 100\%$	rel. wall roughness in %
I	impulse of positive pressure front
$\frac{I D^2}{Q}$	reduced impulse
k_0	scaling factor
k_1	attenuation constant defined in text
k	$D(dp/dx)/P$
l	thickness of plane charge in tube
L	distance charge-observation point
p	side-on front pressure (atm)
p_{so}	unattenuated scaled pressure
p_{20}	pressure at $L/D = 20$
$p_{av}(t)$	averaged pressure-time profile
Q	charge weight (TNT)
t_a	time of arrival of blast front
t_+	duration of overpressure

The success of any physical investigation depends on the judicious selection of what is to be observed as of primary importance, combined with a voluntary abstraction of the mind from those features which, however, attractive they may appear, we are not yet sufficiently advanced in science to investigate with profit.

J. Clerk Maxwell

I. INTRODUCTION

The need for blast load prediction methods in tunnel configurations has long been recognized. This need has become acute because of military underground defence construction projects, civil tunnel constructions for roads and water and transport-tunnels at the factories for explosives.

This report presents the results of a series of experiments on one-dimensional blast wave propagation in steeltubes, diameter 5 cm and 20 cm, in a concrete tube of diameter 80 cm and finally in a tunnel in rock of effective diameter 6 m. The blast waves originated from detonation of TNT charges placed in the center of the tubes/tunnel.

The experimental program was devoted to a study of the validity of common scaling laws and the attenuation of plane blast waves. The discussion and results are presented in rather simple terms intended to give the reader a physical picture of the phenomena which occur. The detailed discussion of the problem would be exceedingly complex and beyond the scope of this report. This report is therefore not claimed to be a strict scientific one, but rather a survey with some rules for thumb for people in charge of planning and design of constructions mentioned above.

II. S C A L I N G

II.1 Dimensional analysis

If all parts of a model have the same shapes as corresponding parts of the prototype, the two systems have geometrical similarity. There is then a point-to-point correspondance between model and prototype.

When numerical values from measurements in model are transformed to the prototype, we must consider the independent variable in the problem. A dimensional analysis of the relationship invariably leads to an equation of the form

$$(II.1) \quad a = f(a_1, a_2, \dots, a_n)$$

where the a 's are a complete set of dimensionless products./1/. In most cases is it impossible to get complete similarity in a model test. Therefore we may let some of the independent variables, which are thought to be of secondary influence on the phenomenons to be investigated, diverge from their correct value.

In two systems - prototype and model - one may choose homologous cartesian systems of axis (x, y, z) and (x', y', z') . Suppose one couples the two systems together such that homologous points and times are defined by

$$x' = k_x \cdot x$$

$$y' = k_y \cdot y$$

$$z' = k_z \cdot z$$

$$t' = k_t \cdot t$$

The constants k_x , k_y and k_z are the scaling factors for the lengths in x , y and z direction. k_t is the time scaling factor.

The general expression for similarity can be defined from two abstract scalar functions $f(x, y, z, t)$ and $f'(x', y', z', t')$:

It is a similarity between the functions f' and f if the ratio f'/f is a constant and the functions are evaluated at homologous points and times. The scaling factor for the function f is:

(II.3) $k_f = f'/f$

In the evaluation of scaling-laws for a system it is often useful to find:

- a) The independent variables which are of importance for the experiment.
- b) Perform a dimensional analysis of the variables and find invariant products.
- c) Find the scaling factor for transformation from model to prototype.

II.2 The principle of similarity in one-dimensional blast wave propagation

The practical importance of the principle of similarity lies in the economy of effort it permits in determining the properties of blast waves and in the predictions it makes possible of the effect of changed scale.

Once the form of a function is found experimentally, pressure say, over a range of either distance or charge size only, its value for other weights or distances is known.

In order to check the validity of this proposition, let us change the scales of measurements of both length L_1 and time t_1 by a factor k_0 , i.e. $L_2 = k_0 L_1$, $t_2 = k_0 t_1$. The principle of similarity

asserts that the pressure and other properties of the blast wave will be unchanged if the dimensions of the charge Q are changed by the same factor k_0 , or referring to fig II.1 the thickness of a plane charge in tube is changed from l_1 to $l_2 = k_0 \cdot l_1$.

This is justified by the fact that the Euler equations and the Rankine-Hugoniot equations describing the blast wave if viscosity and heat conduction can be neglected, are satisfied by all sets of values of L , t and l as the scaling factor k_0 cancels out as all the derivatives are of first order.

This is discussed in detail in ref /2/.

From this we may conclude that if the principle of similarity is true at any value (L_1, t_1) , e.g., pressure $P(r_1, t_1) = P(k_0 r_1, k_0 t_1) = P(r_2, t_2)$, it is true for all values of L and t .

The validity of the principle therefore depends on whether similarity is found to hold true in the initial stages of the explosion.

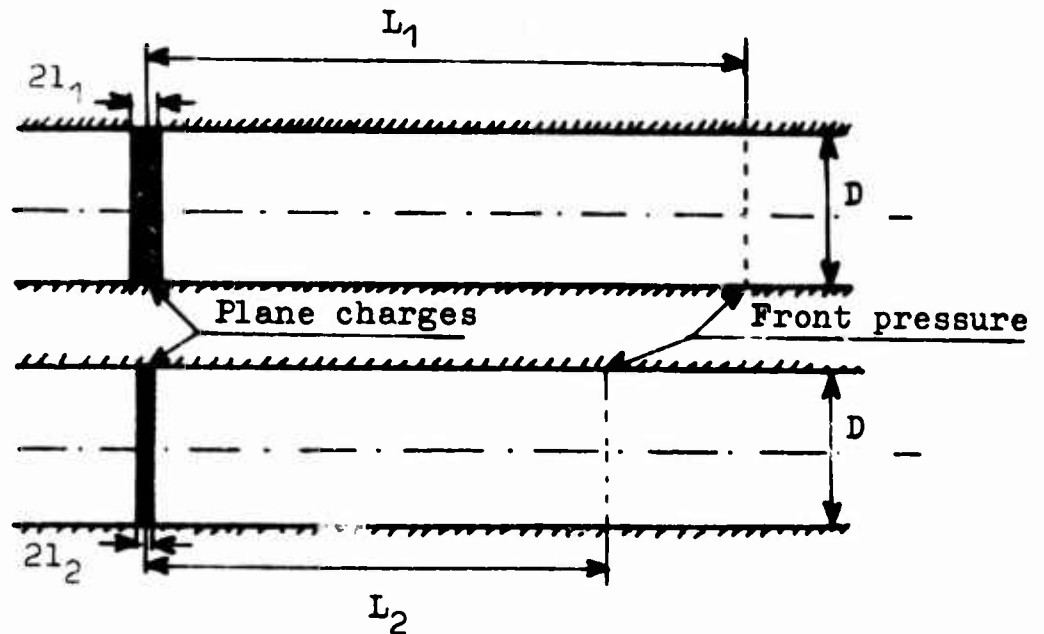


Fig II.1 Plane charges filling the whole tube cross-section

The fact that the pressure and other properties are unchanged if the linear dimensions of the source and scales of length and time are all changed in the same ratio, does not of course specify what the values are without other informations, but experiments may give the functional dependence. The principle can be satisfied only if the pressure depends on distance and time only as a function of the ratios l/L , t/l and hence the front pressure may be expressed as

$$(II.4) \quad p = f\left(\frac{l}{L}\right)$$

Another important property of such a blast wave is the impulse. For unit area of the wave front the impulse I is given by

$$(II.5) \quad I(L, t') = \int_0^{t'} p(L, t) dt$$

where the origin of time is taken to be arrival of blast front at L . The time t' to which the integration is carried out should be taken proportional

to the scaling factor and we write $t' = A \cdot l$ where A is a function only of l/L , and the pressure P depends on L and t only by the ratios l/L , t/l .

hence

$$(II.6) \quad I(L, t') = l \cdot \int_0^{A(\frac{l}{L})} P(\frac{l}{L}, \frac{t}{l}) d(\frac{t}{l})$$

and the integral being a function only of l/L , we obtain

$$(II.7) \quad I(L, t) = l \cdot g\left[\frac{l}{L}, A\left(\frac{l}{L}\right)\right]$$

where g is an undetermined function.

The impulse measured for proportional distance and time scales is therefore proportional to the linear dimension l .

If one detonates a spherical charge, Q , in a tube, the detonation generates a blast wave which more and more gets the character of a one-dimensional wave when it propagates down the tube (fig II.3).

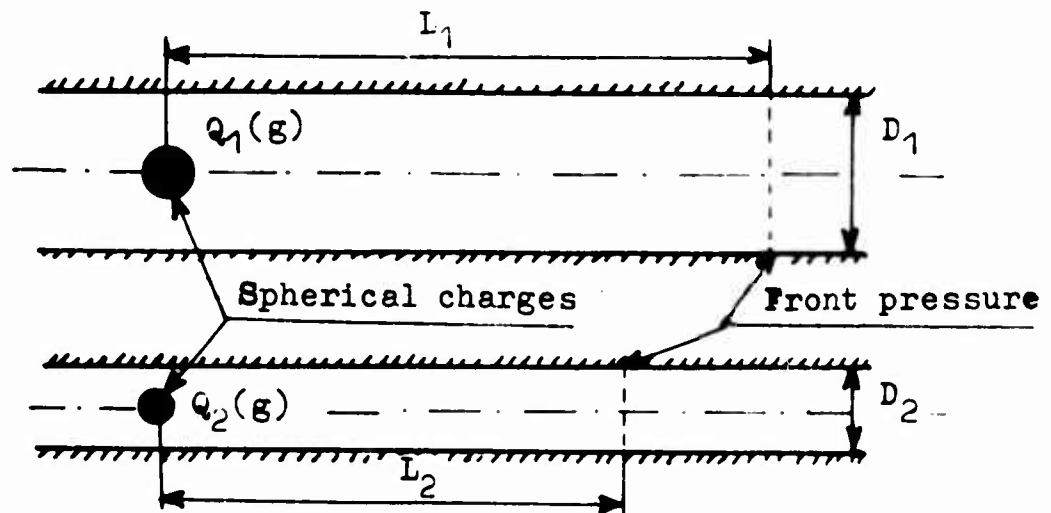


Fig II.2 Spherical charges in tubes

Since the linear dimensions of a charge are proportional to the cube root of the volume and hence weight Q the thickness l in fig II.1 is given as

$$(II.8) \quad 1 \propto \frac{Q}{D^2}$$

From the previous we are now prepared to write the scaling laws for the most important blast wave parameters.

$$(II.9) \quad \text{Pressure:} \quad p = f \left(\frac{Q/D^2}{L} \right)$$

$$(II.10) \quad \text{Impulse:} \quad \frac{I}{Q/D^2} = g \left(\frac{Q/D^2}{L} \right)$$

Positive duration (or duration of overpressure):

$$(II.11) \quad \frac{t_+}{Q/D^2} = h \left(\frac{Q/D^2}{L} \right)$$

Arrival time of pressure front (or time from detonation to blast wave reaches distance L):

$$(II.12) \quad \frac{t_g}{Q/D^2} = i \left(\frac{Q/D^2}{L} \right)$$

Here f , g , h and i are unknown function of Q/LD^2 , (shortened equivalent charge weight Q_E) and may hopefully be determined by experiments.

Experiments on this has been done in Sweden ref. /3/.

II.3 Attenuation in long tunnels.

A blast wave is a physical discontinuity which is propagated through a suitable elastic fluid with a characteristic supersonic velocity M (Mach number). When the medium exhibits energy dissipative effects such as viscosity and thermal conductivity, a reduction in the magnitude of these discontinuities and an increase in the length of the discontinuous region occurs.

An added attenuation is introduced when the blast wave is confined to the interior of a bounded medium such as a tube. The added factor may be separated into two contributions, one being characteristic of the fact that the blast wave

is generated from detonation of more or less spherical charges within the tube itself, and the other being characteristic of the walls and the strength of the blast wave.

The first type of attenuation gives a pressure decrement which is very steep and is in effect the first few tube diameters in traversed distance (fig II.3).

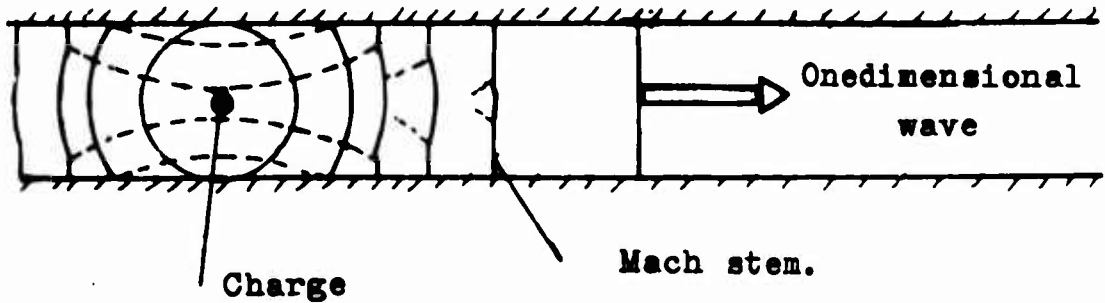


Fig. II.3. Blast wave formation inside a tube

The pressure across the shock front attenuates as it travels down the tube due also to the frictional losses on the walls of the tube. For very short tunnel lengths, i.e. for tunnels whose lengths are not very many times greater than the diameter (or its average cross-sectional diameter for the tunnel) attenuation due to wall roughness is very small. However, for long tunnels having lengths equal to about 30 or more diameters, significant attenuation of the blast wave should be expected. One of the primary aims of this program is to experimentally determine the magnitude of this attenuation.

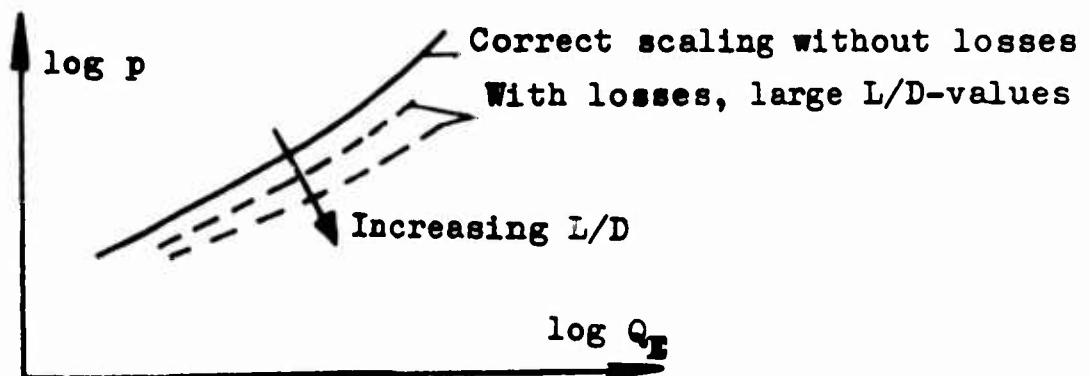


Fig. II.4. Deviation from ideal scaling.

Without wall attenuation and different other dissipative effects for different tubes/tunnels and charges, the experimental points for front pressure versus equivalent charge after eq (II.9) should lie on one smooth curve as shown in fig. II.4. Attenuation due to wall roughness would move this curve with L/D more or less as parameter for one type of tube and roughness. This comes about from principle of similarity described in part II.2, which evidently fails in any circumstances for forces not scaling geometrically. One such force is the effects of viscosity which gives rise to terms of second order derivatives in the equation of motion, and with this the equation of motion is not satisfied on substituting $p(k_0 L_1, k_0 t_1)$ etc for $p(L_1, t_1)$ etc.

At the last front, processes similar in effect to macroscopic viscosity and thermal conduction must be significant, but this turns out to be of no practical significance to the applicability of the principle of similarity.

For the tunnel the effective diameter is taken as $D = (4A/\Pi)^{1/2}$, where A is the tunnel area. applicable for scaling of length in frictionless flow. Friction effects, however, depend on the length of the tunnel periphery C in contact with the moving gas, and the effective diameter is more properly C/Π . In our case, however, the tunnel diameter was not defined better than difference between the two definitions because of somewhat varying tunnel diameter.

III. TEST PROGRAM

III.1 General

The tubes used were chosen as to make a rough test of the validity of common scaling laws. As our Office of Test and Development neither had the money nor the time to make extensive tests, only steeltubes of diameter 5 and 20 cm, a concrete tube of diameter 80 cm and a tunnel in rock of effective diameter 600 cm with constant roughness for each tube/tunnel were used.

General test descriptions for these series of experiments are tabulated in table III.1.

Tube/Tunnel	Steel	Steel	Concrete	Rock
Diameter D(cm)	5	20	80	600
Wall rough- ness e/D 100%	0,5% ($e \approx 0,26$ mm)	0,13% ($e \approx 0,26$ mm)	0,03% ($e \approx 0,2$ mm)	8% ($e \approx 0,5$ m)
Charges TNT (g) between ^{x)}	1,5-17,5	1,5-200	9,5-5000	21,5-92300
Distance charge - meas. L/D between	6,4-705,2	4,5-150,7	4,85-100,5	2,92-38,33
Side-on over- pressure p(ato) between	0,2-77	0,2-32	0,07-23	0,005-1,5

x) Electrical detonation cap no 8, equivalent TNT charge 1,5 g included.

Table III.1. Test description



Fig II 5. 80 cm diameter concrete tube at test site.



Fig II 6. 5 cm diameter steel tube with transducer mounting and arrangement for time of arrival measurements.

Pencilshaped Lead Zirconate transducers were used in conjunction with an oscilloscope and polaroid camera to measure pressure-time history. These transducers were centermounted in the tubes/tunnel.

Fig II.5 shows the 80 cm diameter concrete tube and II.6 a portion of the 5 cm diameter steel tube.

III.2 Roughness of tubes and tunnel in rock

Tunnel wall roughness was estimated by taking the percentage of the ratio e/D , where e is the roughness particle diameter and D is the tube/tunnel diameter.

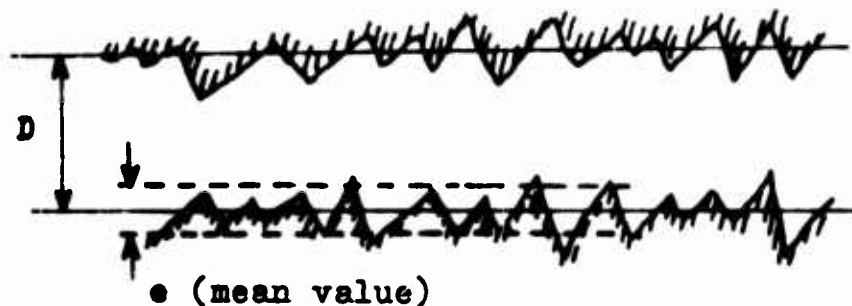


Fig.III.1. Definition of roughness $\frac{e}{D} \cdot 100\%$

As for the steeltubes the roughness originated from corrosion. For the concrete tube the roughness was the standard production roughness for PREMO-tubes, manufactured at A/S Dalen Portland-Cementfabrik, Brevik, Norway.

The tunnel used was an abandoned railway tunnel with raw-detonated rock. The tunnel had a curvature of radius approximately 100 m. It is thought that the effect of this bend can be neglected and the tunnel may be considered as being straight.

III.3 Explosive charges

The explosive used were cylindrical pressed TNT charges with a hole drilled along the cylinder-axis to fit the electrical detonation cap no 8.

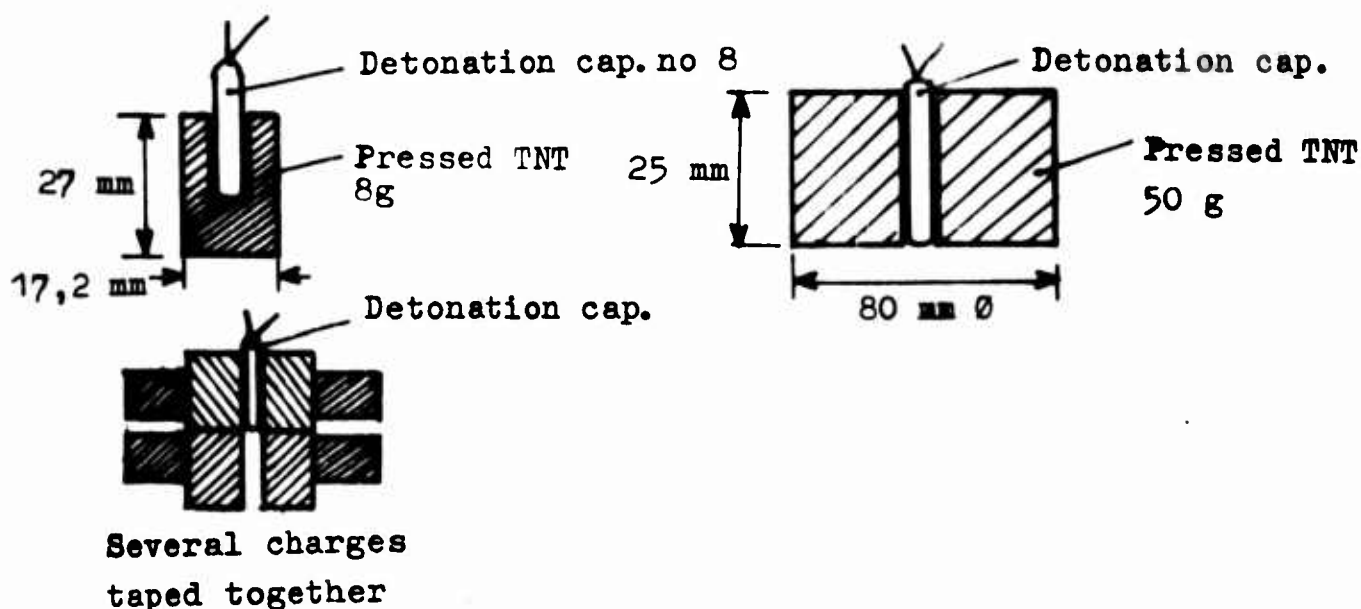


Fig III.2. Typical TNT-charges used

In a series of calibration tests the electrical detonation cap was found to be 1,5 g equivalent TNT charge as regards front pressure.

The charges were hanging in center of tube in a string going through a small hole on the upper side of the tube. In the tunnel tests the heavier charges were placed on a wooden platform as to be placed roughly in the center of the tunnel. The different shaped charges is not believed to have had any significant influence on blast waves at longer distances ($L/D \gtrsim 5$).

III.4 Transducers

The gages used were type LC-33, from Atlantic Research Corporation. This is a pencilshaped Lead Zirconate and side-on pressure measuring type transducer. The nominal characteristics in table III.2. Typical pressure time profile from test in shock tube is shown in fig.III.4.

The transducers were calibrated at the factory to within $\pm 1\%$ reproducibility in the pressure range from 1,7 ato to 13.6 ato.

A best fit calibration curve was used by the computer in evaluation of frontpressure and impulse. Up to 5% uncertainty in calibration was deemed adequate in view of the larger errors introduced in interpreting the oscillographs.

Model LC-33

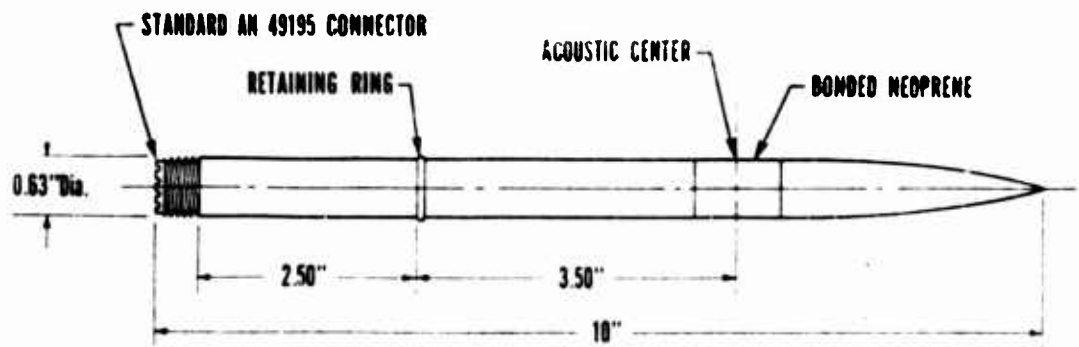
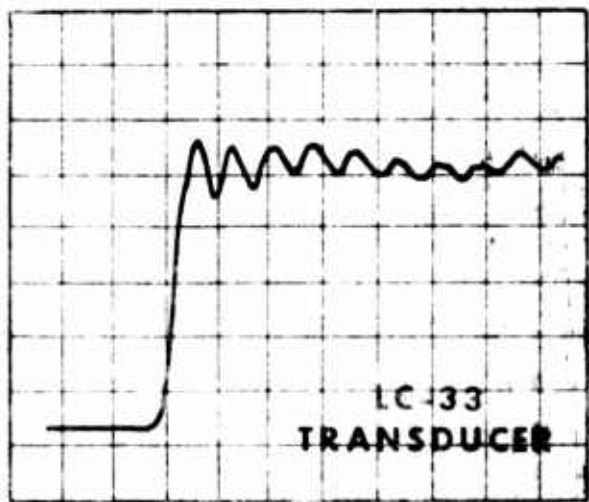


Fig III.3. Dimensions of LC-33 transducer

Table III.2

NOMINAL CHARACTERISTICS

Open Circuit Receiving Sensitivity (1 Kcps)	
db reference 1 volt/microbar	-101
Volts/psi	0.6
Charge Sensitivity (micromicrocoulombs/psi)	2500
Frequency Response, flat +2 db	1 cps to 80 Kcps
Capacitance (microfarads)	0.004
DC Resistance (megohms)	>500
Maximum Static Pressure (psi)	>500
Maximum Transient Pressure (psi)	~1000
Temperature Range (°C)	-40 to +100
Linearity	
Pressure +2% (psi)	100
Temperature +3% (°C)	-60 to +70



ORIENTATION. FACE ON
MEDIUM. NITROGEN GAS
PRESSURE 38 PSI
VERTICAL 5.0 V/div
HORIZONTAL 0.02 ms/div

Fig III.4 TYPICAL PRESSURE-TIME PROFILE

III.5 Transducer mounting

The way in which the gage was mounted in the 5 and 20 cm tube is shown in fig. III.5

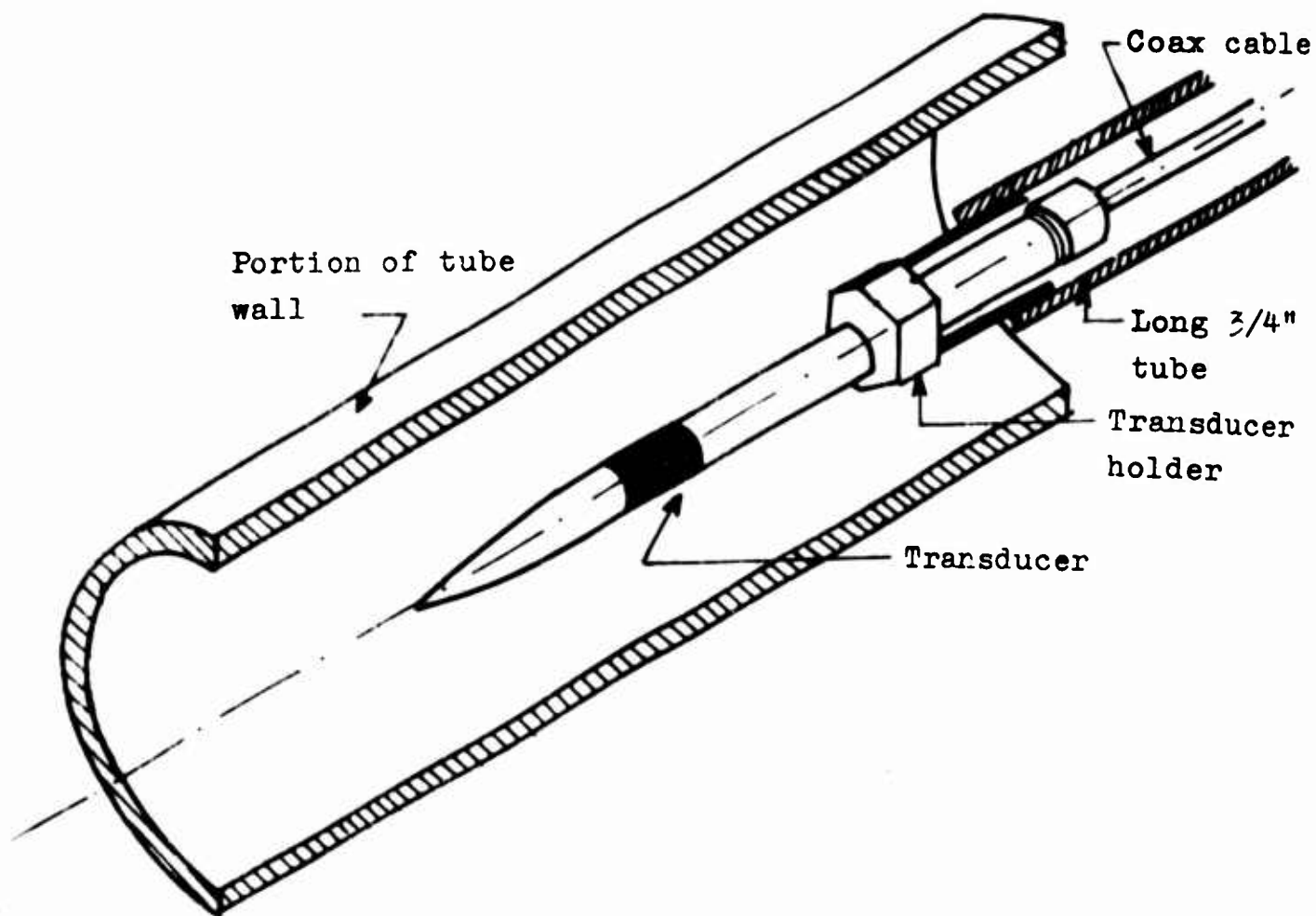


Fig.III.5. Transducer mounted in 5 and 20 cm tube

For the 5 cm and 20 cm tube only one transducer was mounted in the same tube, but as for the 80 cm tube four were mounted at the same time, fig.III.6.

The transducer body and mounting tube are of appreciable diameter compared with that of the smallest tube tested. The area constriction due to the 3/4-in. mounting tube in this case is about 14 percent. The presence of a gage can locally affect the peak pressure and impulse under these conditions.

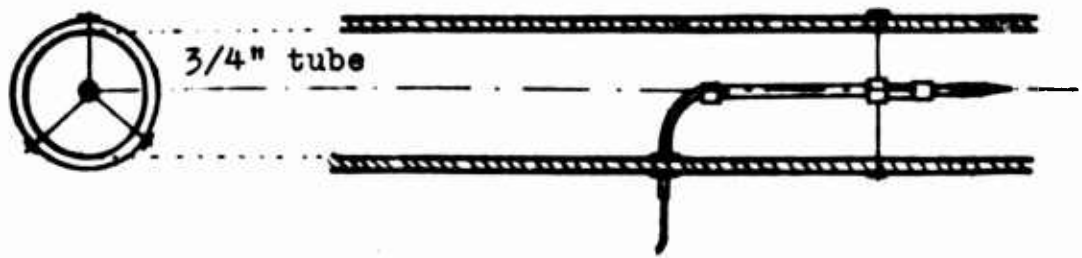


Fig III.6. Transducer mounted in 80 cm tube

In the tunnel 5 transducers were mounted at the same time as shown in fig.III.7.

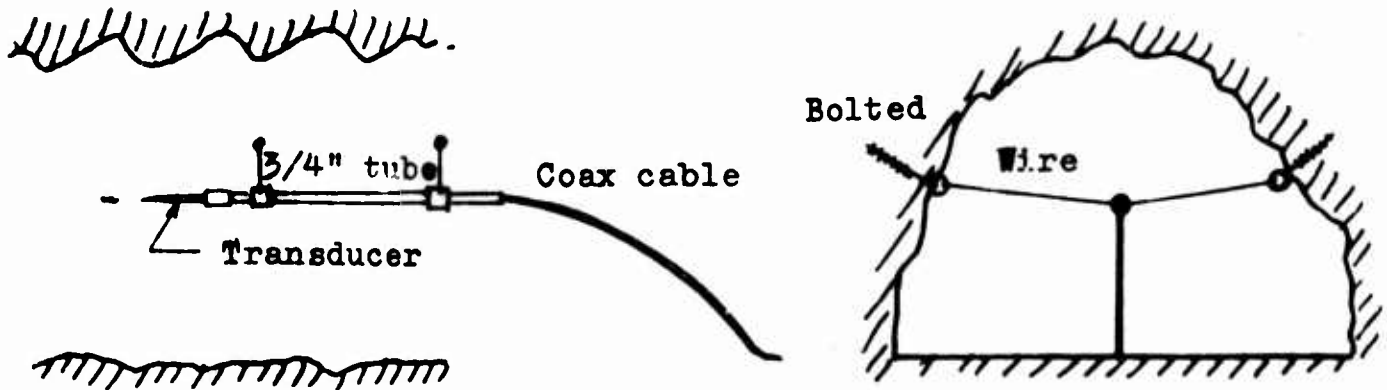


Fig III.7. Transducer mounted in 6 m tunnel in rock

III.6 Instrumentation

The electrical arrangement shown in fig III.8 was followed for the 5 and 20 cm tubes. The Kistler Charge Amplifier (Model 566) served in most cases to match the high impedance of the transducer ($> 10^8$ ohm) to the oscilloscope, a Tektronix Model 502 A. A Polaroid type oscilloscope camera recorded the trace. In many cases a large capacity served as a timeconstant increasing device.

Triggering was done by taping a loop of insulated wire around the charge. In detonating the charge, a well-defined break of wire is obtained. The uncertainty in triggering is estimated to less than $500 \mu s$.

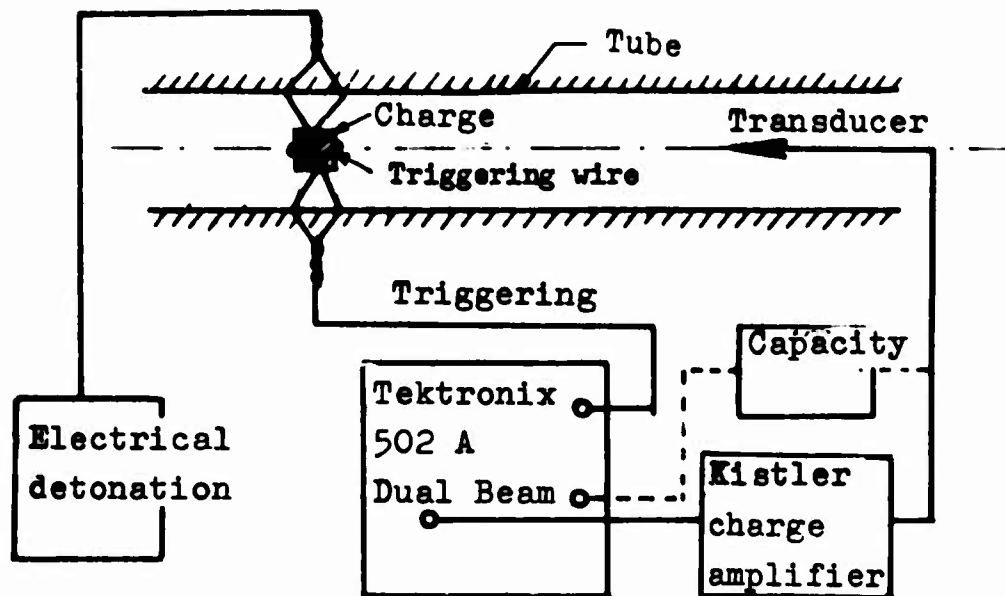


Fig III.8. Schematic electrical flow chart for 5 and 20 cm diameter tube tests

For the less transient blast waves in the 80 cm tube and 6 m tunnel, a CEC recording oscillograph (Consolidated Electrodynamics) was used with preferably fluid damped galvanometers type 7-363, fig III.9. The galvanometer has the following specifications:

Undamped natural frequency	1670 Hz
Flat (5%) frequency range	0-1000 Hz
Undamped DC sensitivity	2 mA/inch
Terminal resistance	69 ohm

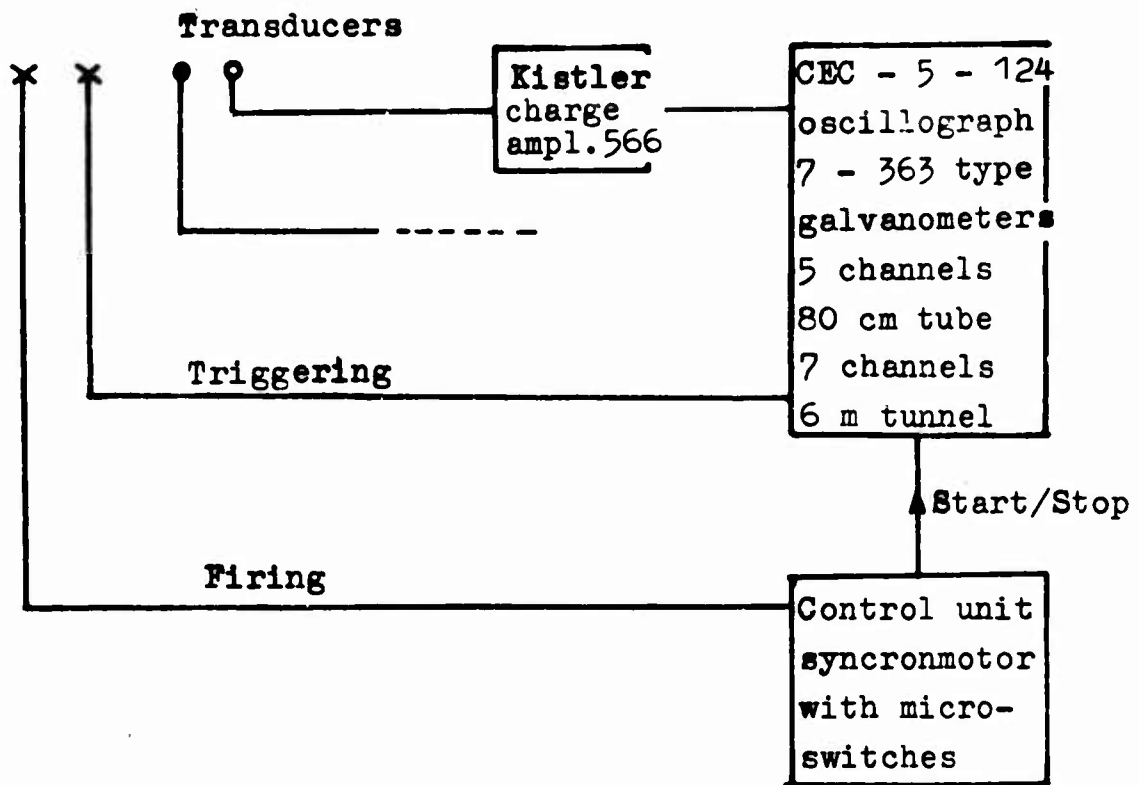
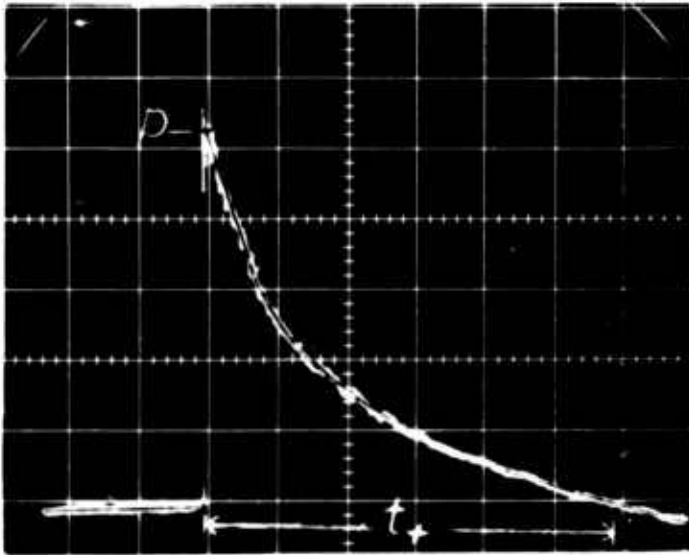
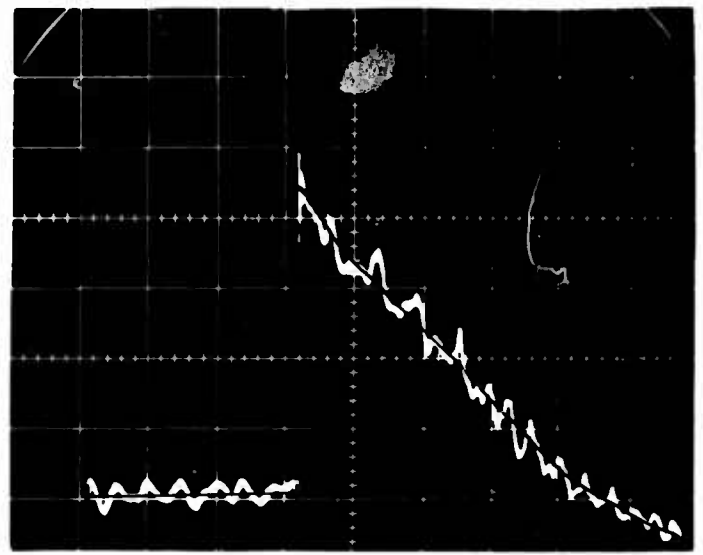


Fig III.9. Schematic electrical flow chart for
80 cm tube and 6 m diameter tunnel
in rock tests

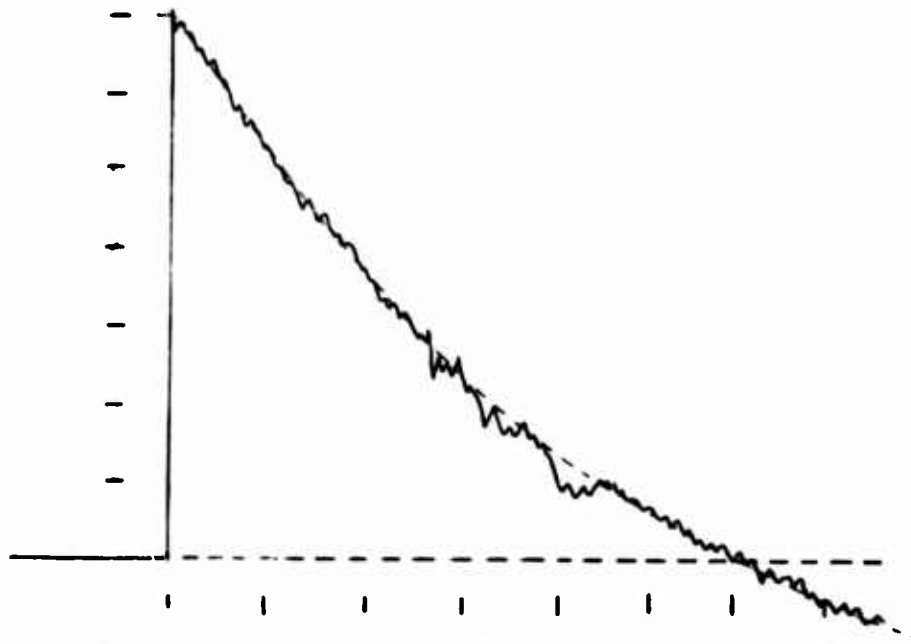
Typical records from oscilloscope and oscillograph
is shown in the reproductions in fig III.10.



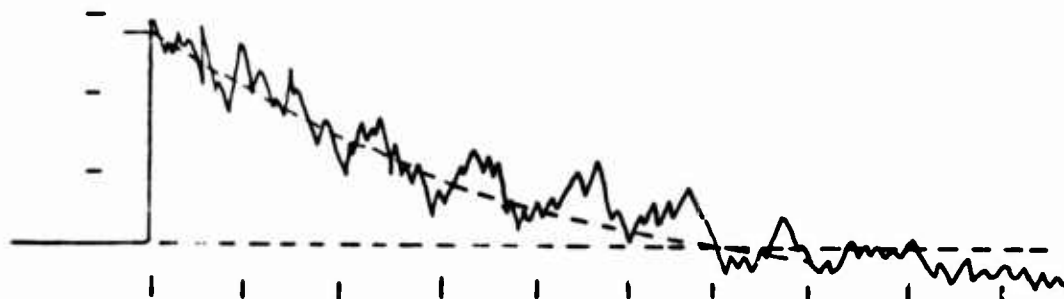
$D = 5 \text{ cm}, L = 1272 \text{ cm}$
 $Q = 9,5 \text{ g TNT}$
 $X = 1 \text{ ms/div}, Y = 0,38 \text{ ato/div}$



$D = 20 \text{ cm}, L = 587 \text{ cm}$
 $Q = 25,5 \text{ g TNT}$
 $X = 1 \text{ ms/div}, Y = 0,67 \text{ ato/div}$



$D = 80 \text{ cm}, L = 44,85 \text{ m}, Q = 500 \text{ g TNT}$
 $X = 100 \text{ ms/div}, Y = 0,088 \text{ ato/div}$



$D = 6 \text{ m}, L = 27 \text{ m}, Q = 7 \text{ kg TNT}$
 $X = 100 \text{ ms/div}, Y = 0,23 \text{ ato/div}$

Fig.III.10 Typical records from oscilloscope and oscillograph

III.7 Check of frontpressure with time of arrival measurements

As frontpressure is uniquely determined from tabulated blast velocity data, a simple check of frontpressure measurements from pressure-time records is possible by simple velocity measurements. This was done with the 5 cm diameter tube. 5 mm diameter holes were drilled through the wall with approximately 20 cm interval and selfmade folioswitches were taped over the holes and contact-time interval was recorded by a Hewlett-Packard counter. Comparison of the two methods is done in fig. III.11, and the difference is not more than expected from the time of arrival measurements.

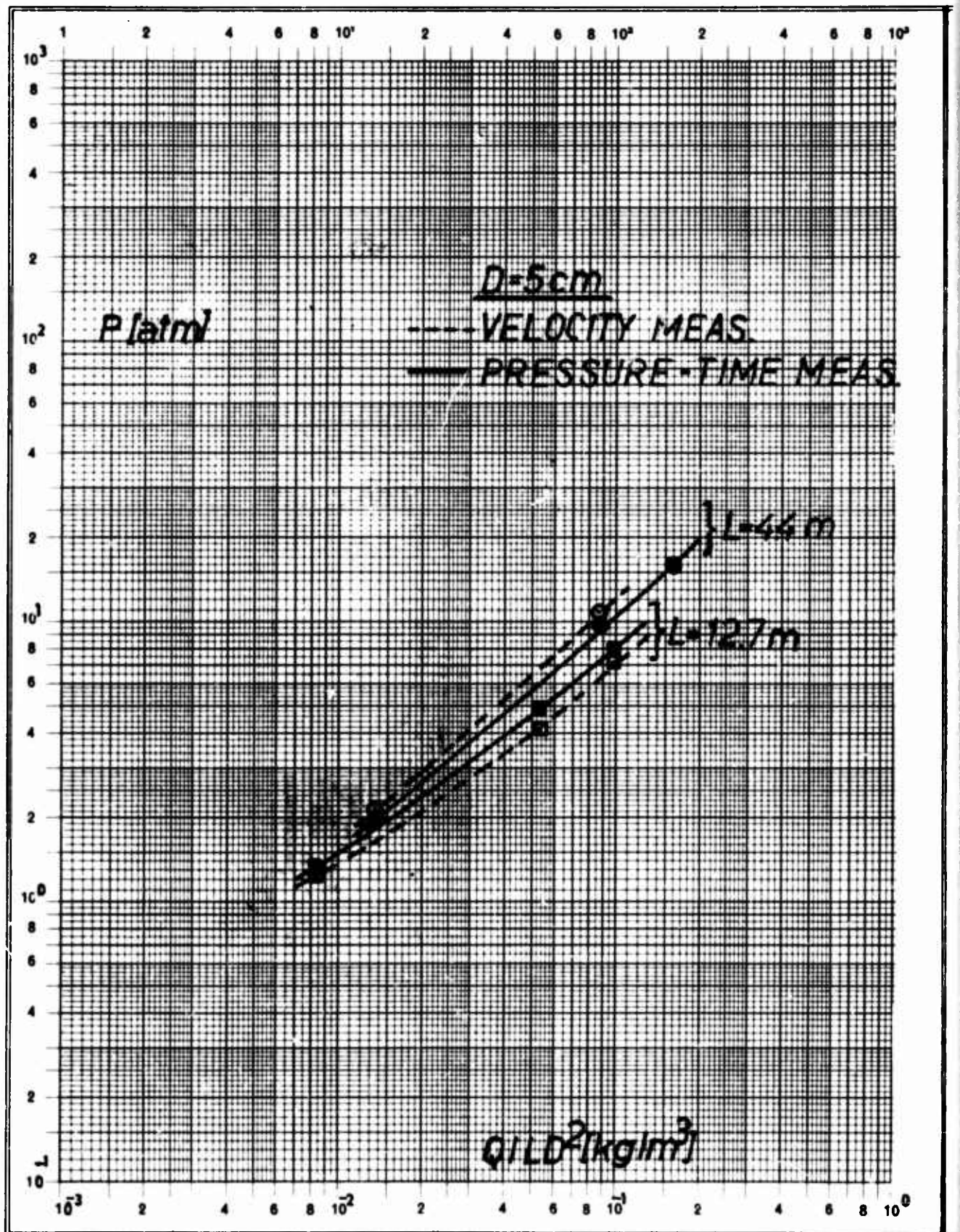


Fig.III.11 Comparison pressure-time measurements and velocity measurements in 5 cm tube

IV. PREPARATION OF DATA

IV.1 Interpretation of traces

As can be seen in fig III.10 the records possessed an irregular pressure-time trace, because of noise, irregularities in the blast wave because of non-ideal one-dimensional flow, overshoot in transducer, oscillograph etc. The records were then "averaged" by drawing a best fit smooth curve. However, the determination of pulse height by this method is estimated to give at least 5% uncertainty. For the determination of the impulse the uncertainty is even more, approx. 20% partly because the positive duration, t_+ , is very uncertain. Definitions are given in fig IV.1.

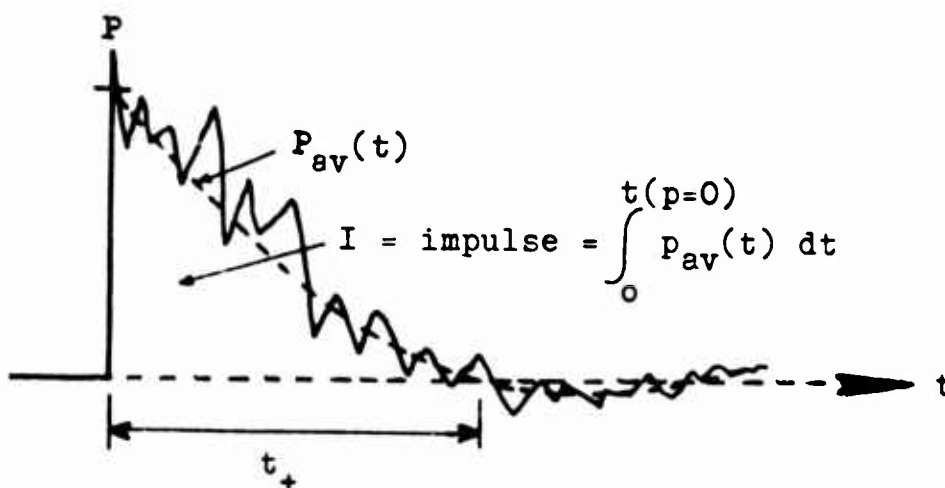


Fig IV.1. Definition of parameters

IV.2 Conversion of pictures to paper-tape

The method for conversion of the pressure-time traces to paper-tape is described in detail in ref /6/. The technique is quite simple and is shown schematically in fig. IV.2.

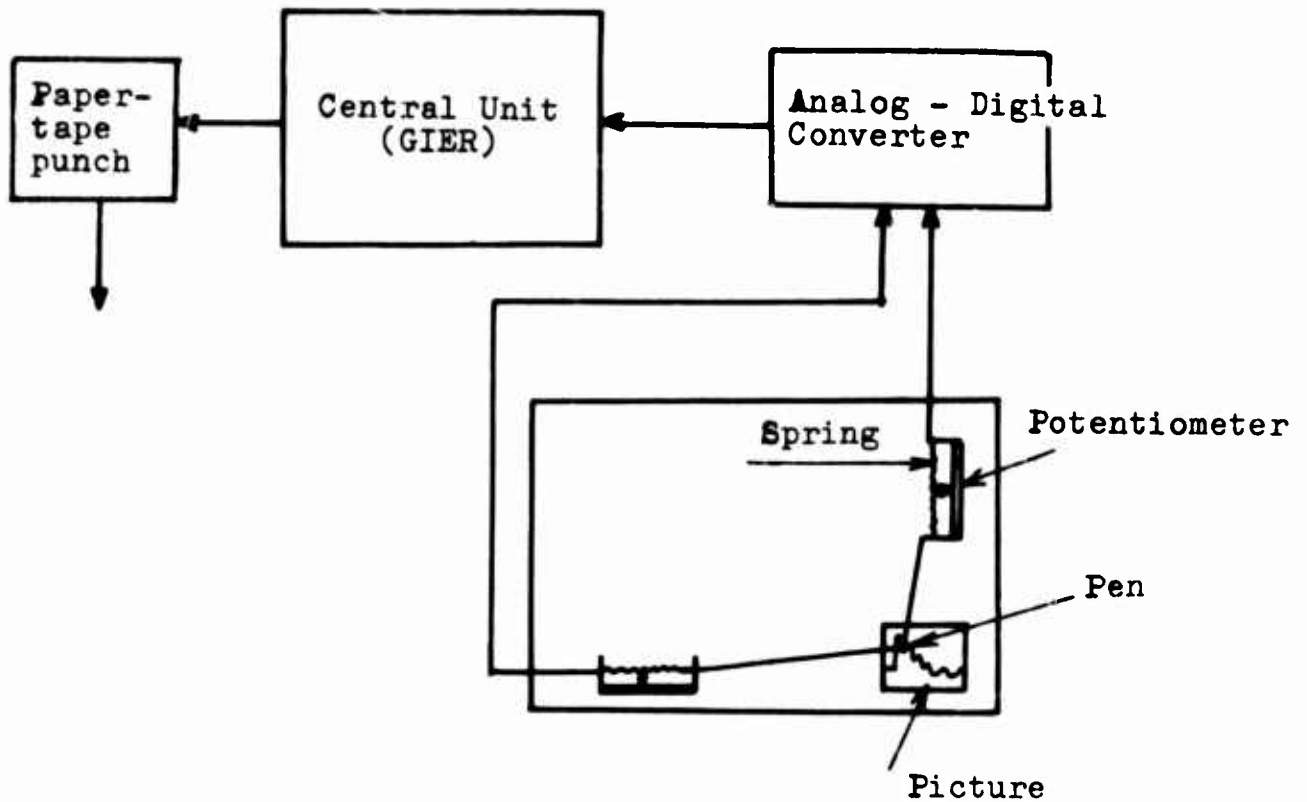


Fig IV.2. Schematic conversion of pictures to paper-tape

Two potentiometers give voltages which is a measure of the x- and y-coordinates of a sufficient chosen number of discrete points on the averaged trace (typical 20 points were chosen).

IV.3 computer work

The further modification of converted data, main programs etc. are too lengthy to be described in detail here, but some features will be mentioned. The computing was done with an UNIVAC 1107.

The frontpressure P was picked out as the largest ordinate.

The impulse of positive pressure front:

$$I = \int_0^{t_+(p=0)} p_{av}(t) \cdot dt$$

was computed with common trapezoid-integration.

t_+ was found as time from pressurefront to averaged pressure curve again reaches zero.

V. RESULTS AND DISCUSSION

V.1 Frontpressure

Fig V.1 to V.5 presents the data relating the observed front overpressure p to tube/tunnel position in L/D units with TNT charge weight as parameter.

From this is it clear that for the same tube, the higher the peak pressure, the greater the blast-wave attenuation.

At longer L/D distances the results demonstrate that the attenuation is described roughly by

$$(V.1) \quad p = C(p_0)(L/D)^{k_1(p_0)}$$

Taking the initial pressure p_0 at $L/D=20$, we may find the constants $k(p_{20})$ from the averaged curves in fig V.5, (by extrapolating straight lines backwards to $L/D=20$ for the 5 cm tube).

This is shown in fig V.6. For $p_{20} \gtrsim 1$ atm the functional dependence of k_1 is described by

$$(V.2) \quad k_1 \approx -0,433 \log p_{20} - 0,653$$

and

$$(V.3) \quad C \approx 6,79 \cdot p_{20}^{1,61}$$

hence

$$(V.4) \quad p = 6,79 p_{20}^{1,61} \left(\frac{L}{D}\right)^{-0,433 \log p_{20} - 0,653}$$

This is shown in fig V.6 and V.7 to be rough approximations for the 5, 20 and 80 cm diameter tubes for p_{20} in the region 1 to 200 atm (extrapolated back from "long range attenuation" whereas for the attenuation tunnel in rock and $p_{20} \lesssim 1$ atm for the 80 cm diameter tube we do not have this simple functional dependence.

The exponent k seems to reach a more or less constant value for $p_{20} \lesssim 0,5$ atm.

As stated before, it is evident that attenuation is a function of the relative wall roughness, i.e. dependent on the parameter $\frac{e}{D}$. Within the experimental uncertainty one would not expect significant difference in attenuation for the steeltubes and the concrete tube. ($\frac{e}{D}$ between 0,03% and 0,5%). This is confirmed in fig V.6. The tunnel in rock with roughness $\frac{e}{D} \approx 8\%$ seem to give more attenuation in the pressure region of overlapping, i.e. $p_{20} \approx 0,1 - 1 \text{ atm}$.

Additional experiments with systematic change of roughness in one tube and comparison of different tubes with varying diameter are hoped to be the next step in our series of experiments.

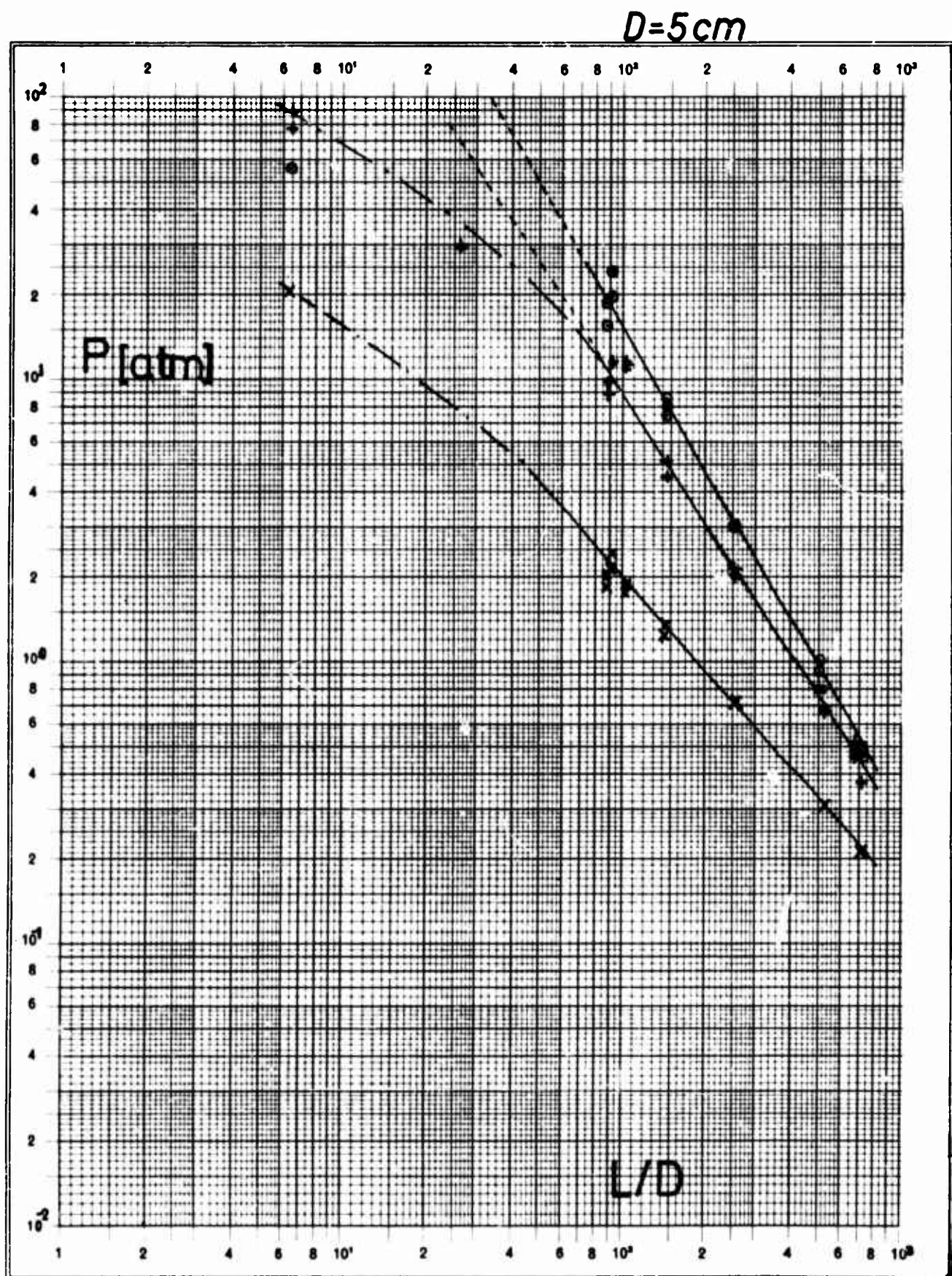


Fig.V.1 Front pressure versus tube position in L/D units
in 5 cm tube

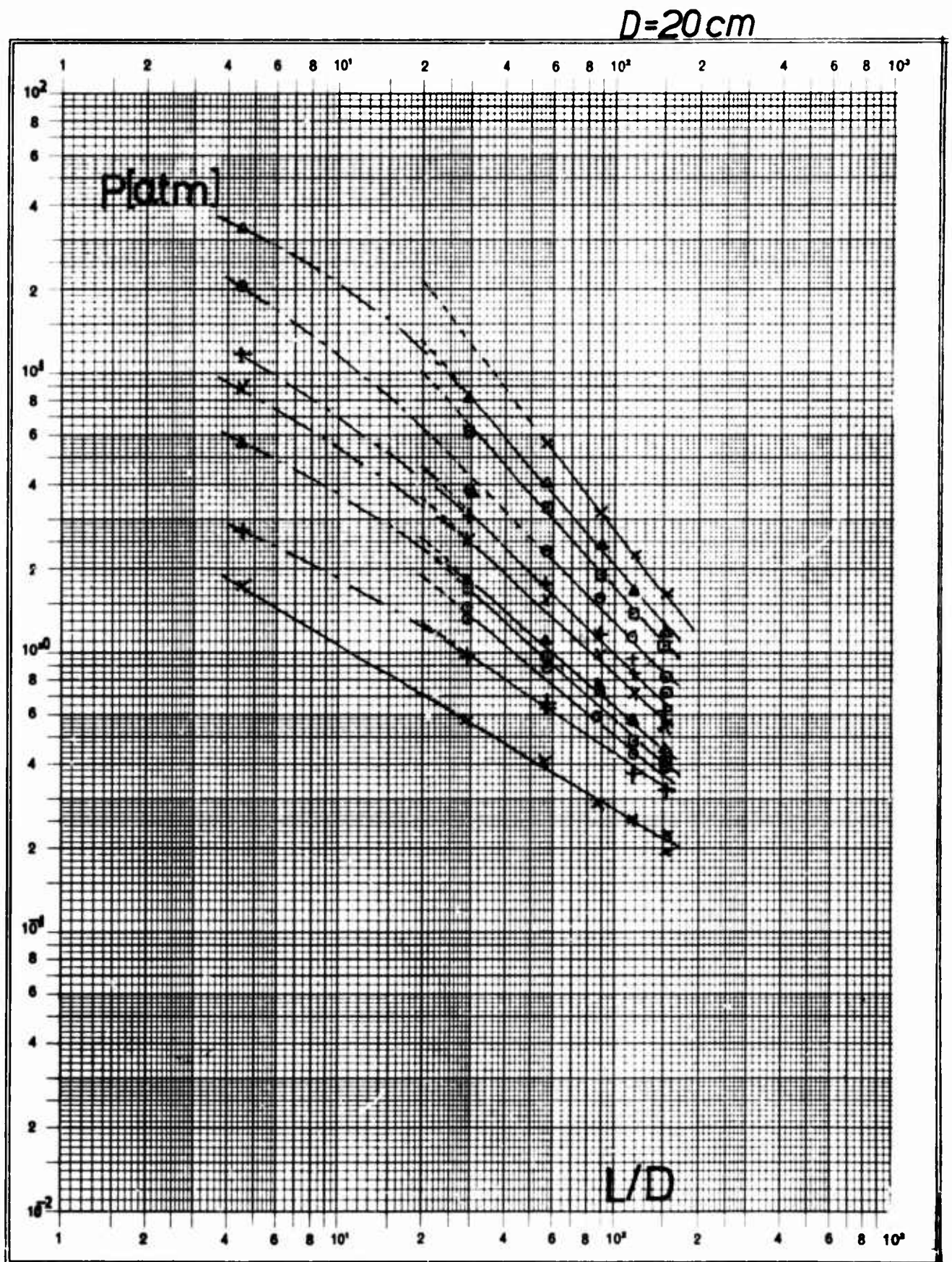


Fig.V.2 Frontpressure versus tube position in L/D units
in 20 cm tube

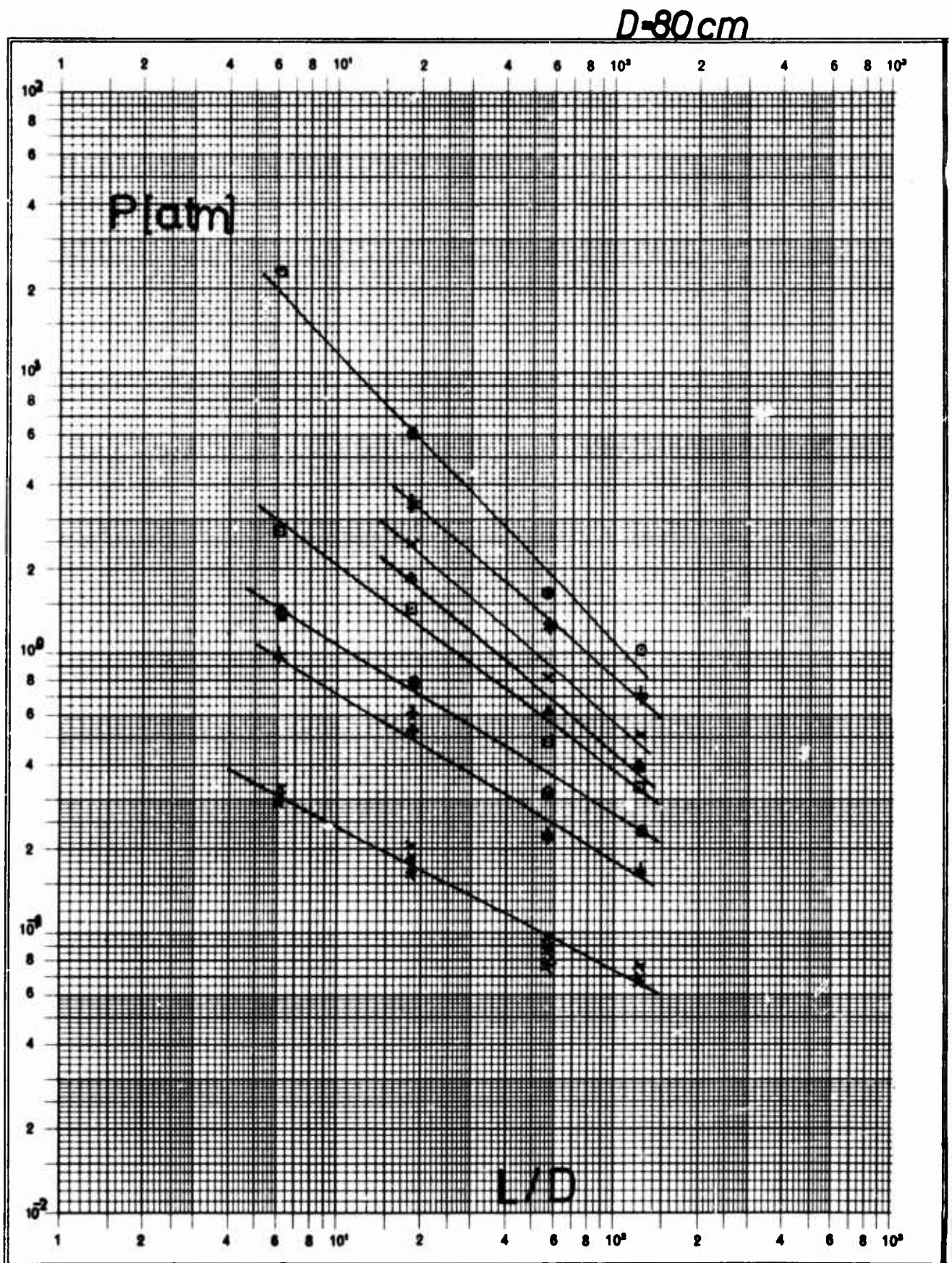


Fig.V.3 Frontpressure versus tube position in L/D units
in 80 cm tube

$D=600\text{cm}$

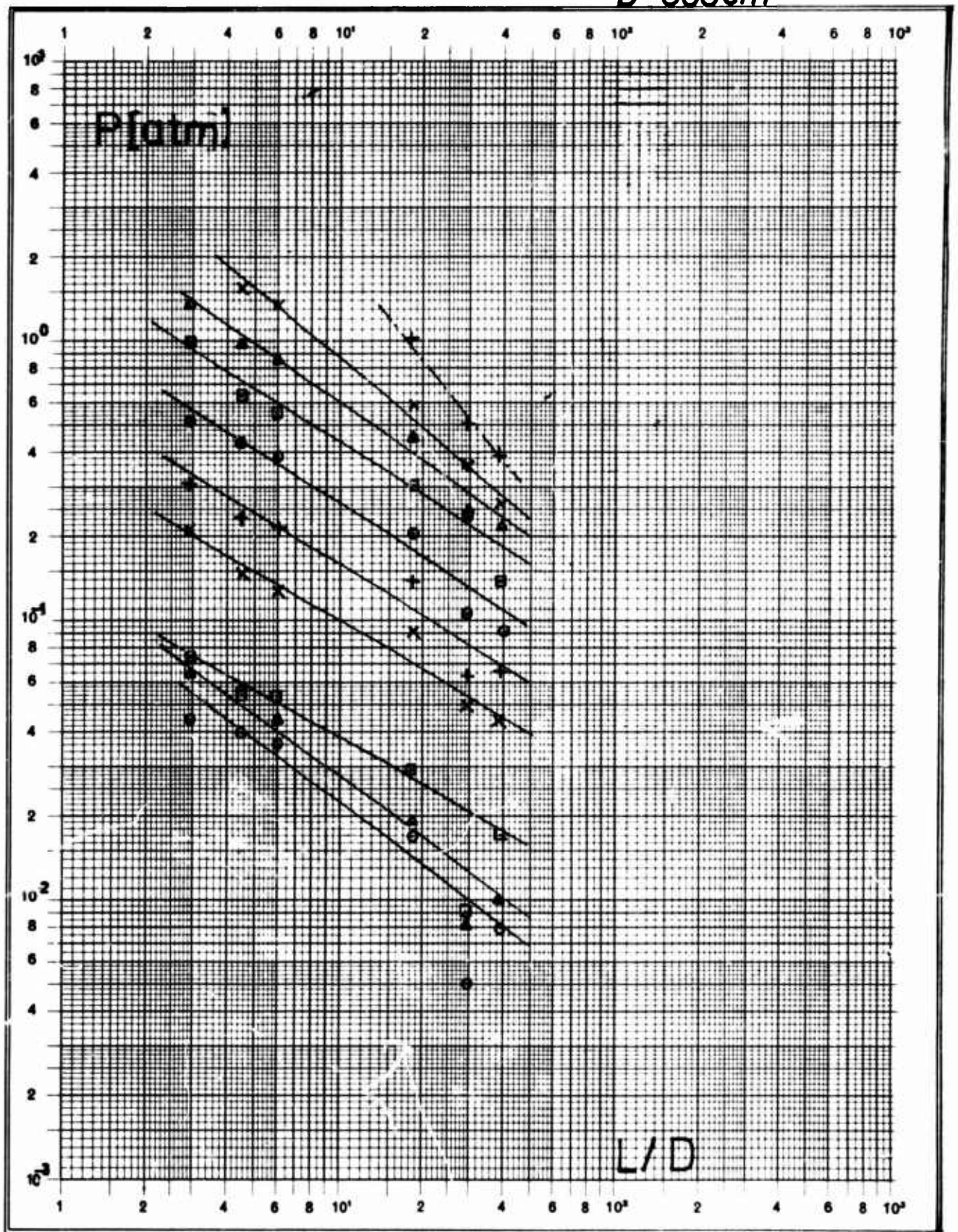
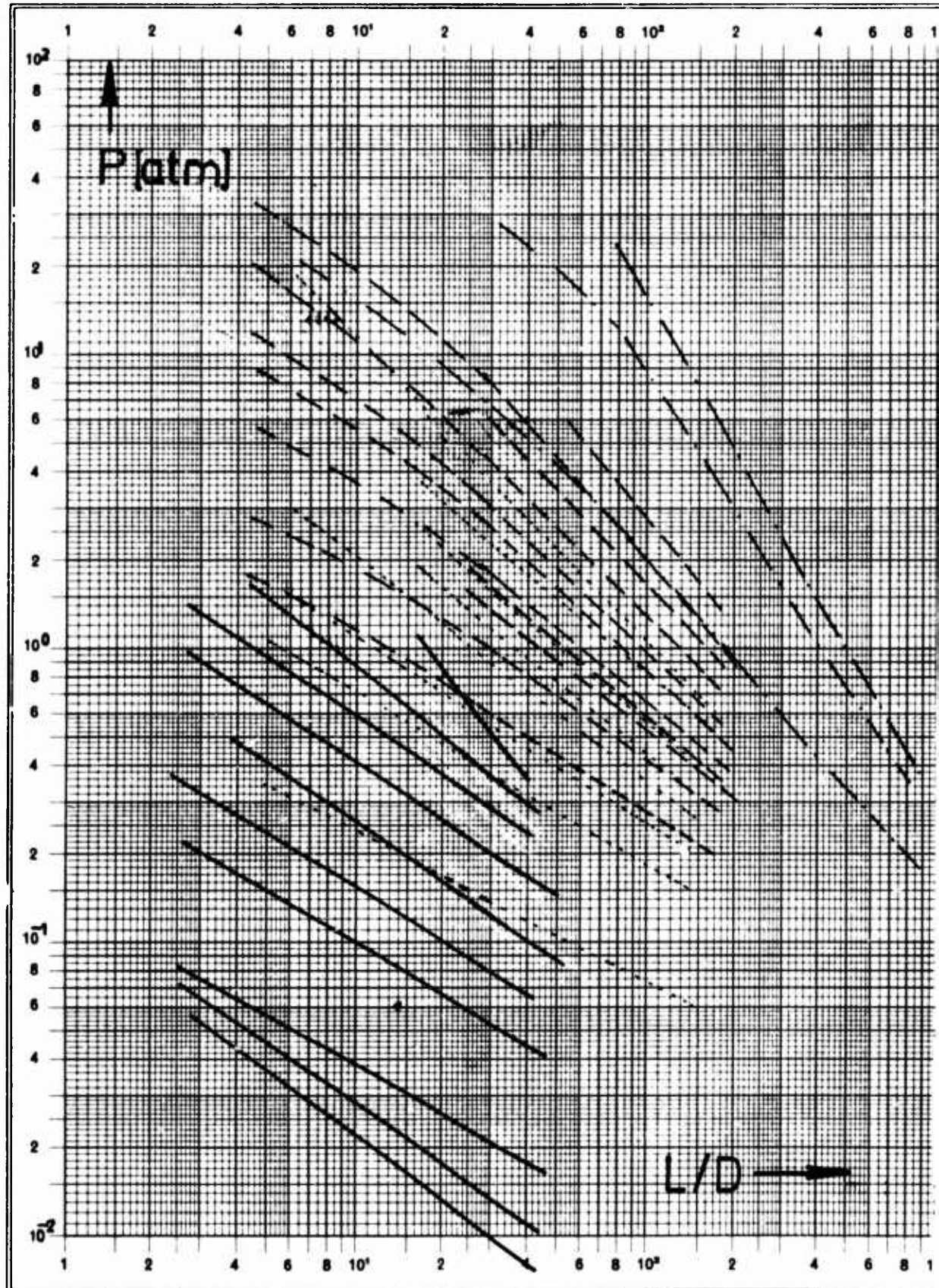
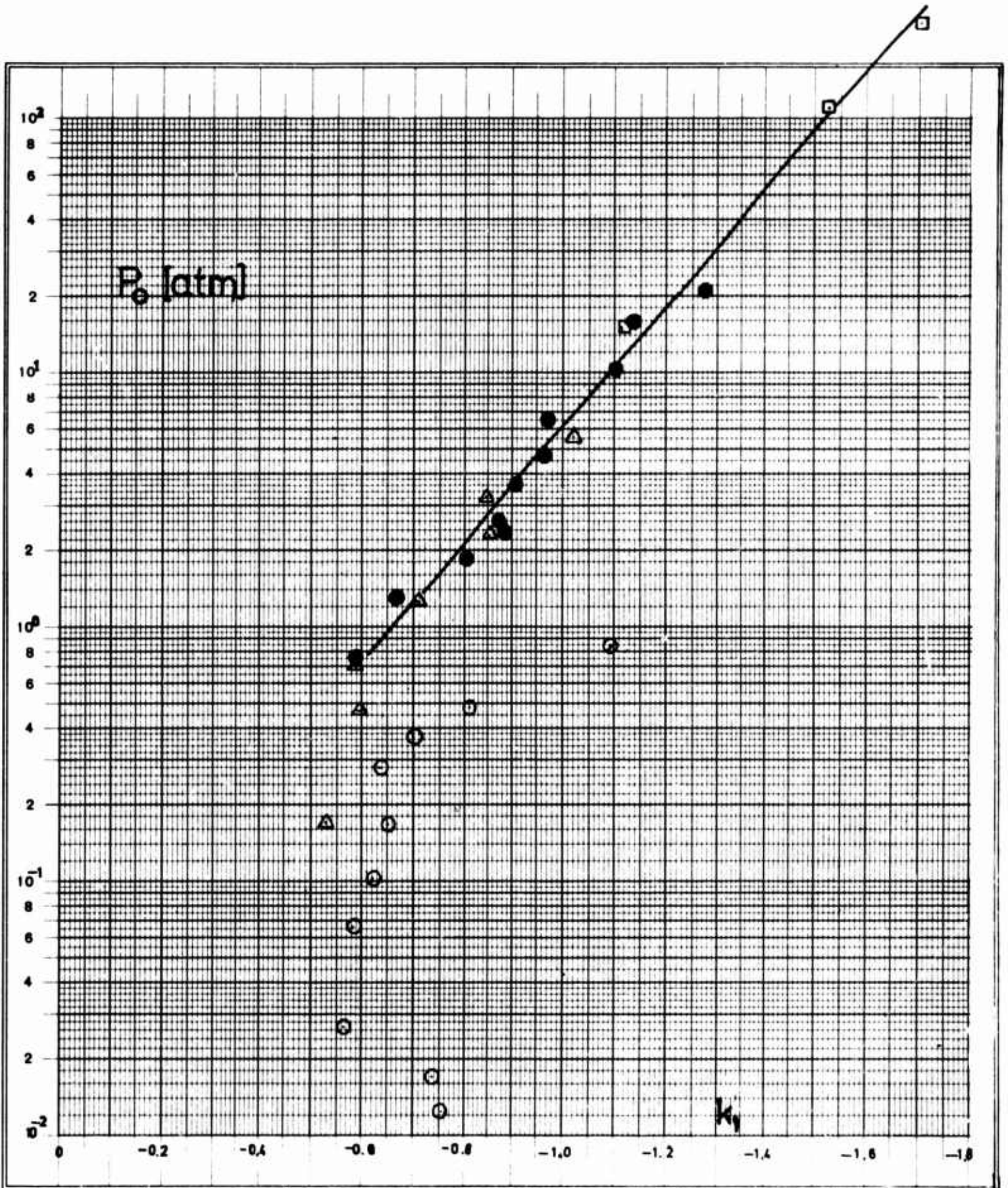


Fig.V.4 Frontpressure versus tunnel position in L/D units
in 6 m tunnel in rock



$D [\text{cm}]$
 --- 5
 - - - 20
 80
 ——— 600

Fig.V.5
Comparison of front pressure
attenuation for different
tubes and tunnel in rock



- $D=5$ cm
- 20
- ▲ 80
- 600

Fig.V.6 Attenuation constant k_1 for longrange attenuation versus initial front pressure p_{20} at $L/D = 20$ from figures V.4 to V.5

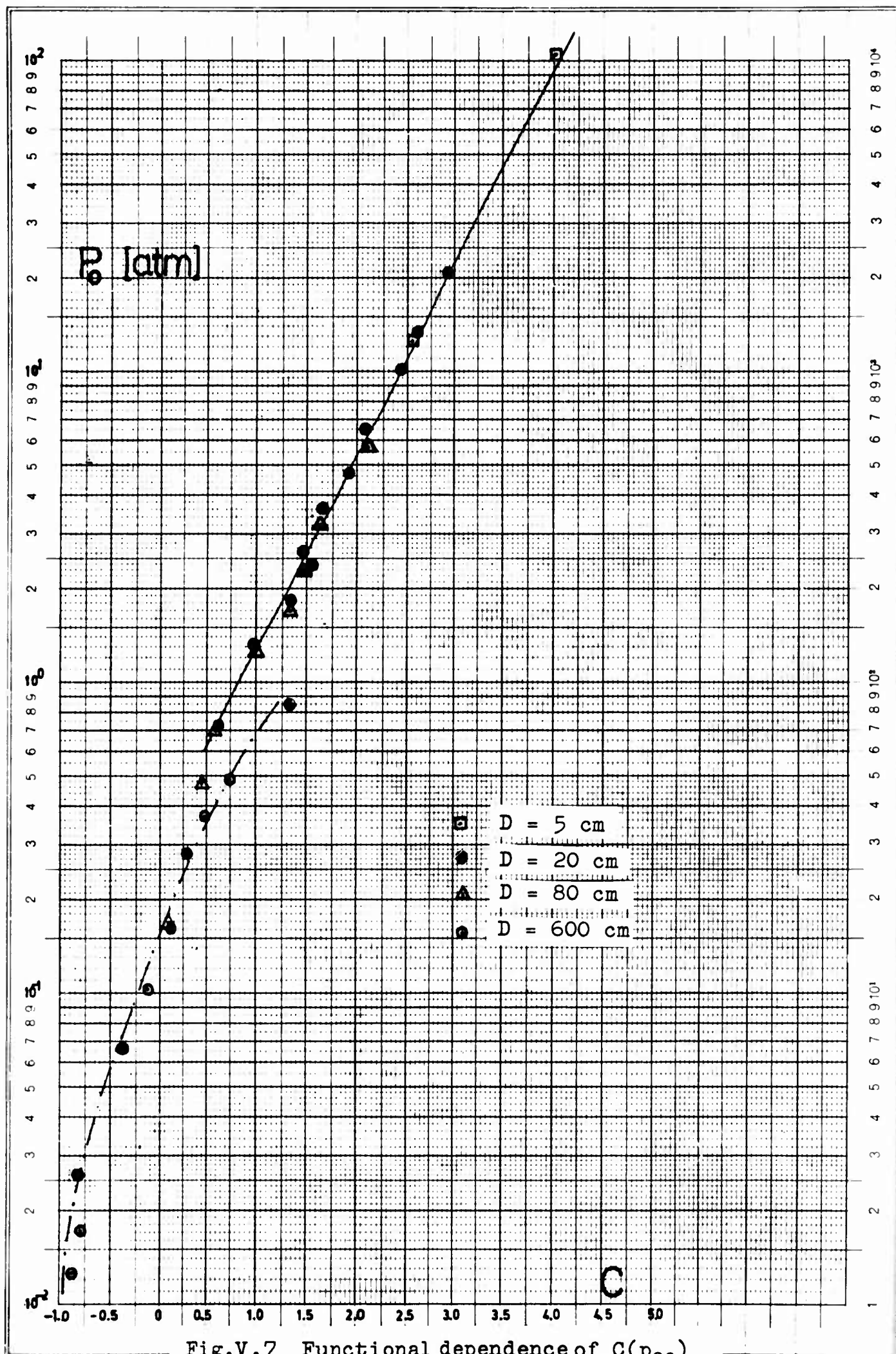


Fig.V.7 Functional dependence of $C(p_{20})$
in eq. $p = C(p_{20}) \frac{L}{D} \frac{1}{K(p_{20})}$

Checking of the validity of the scaling law proposed in chapter II.2 eq (II.9) for the front pressure

$$(II.9) \quad p = f\left(\frac{Q}{LD^2}\right) = f(Q_E)$$

is shown in figures V.8 to V.12.

The 5 cm tube results in fig V.8, 20 cm in fig V.9, 80 cm in fig V.10 and the 6 m tunnel in rock in fig V.11. The influence of the wall attenuation clearly manifests itself in the lowering of the pressure curves with increasing L/D values. Direct comparison of all data is given in fig V.12.

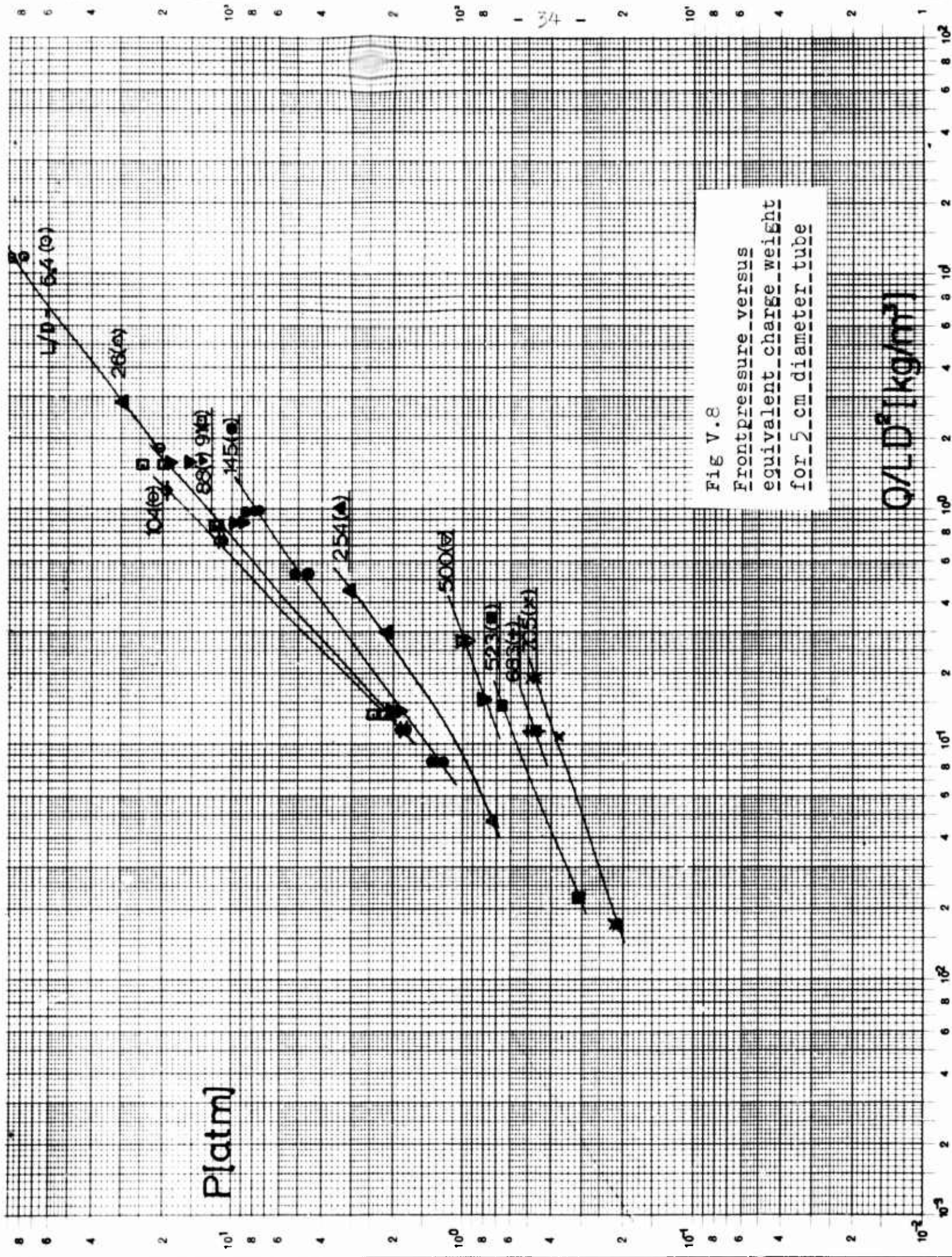


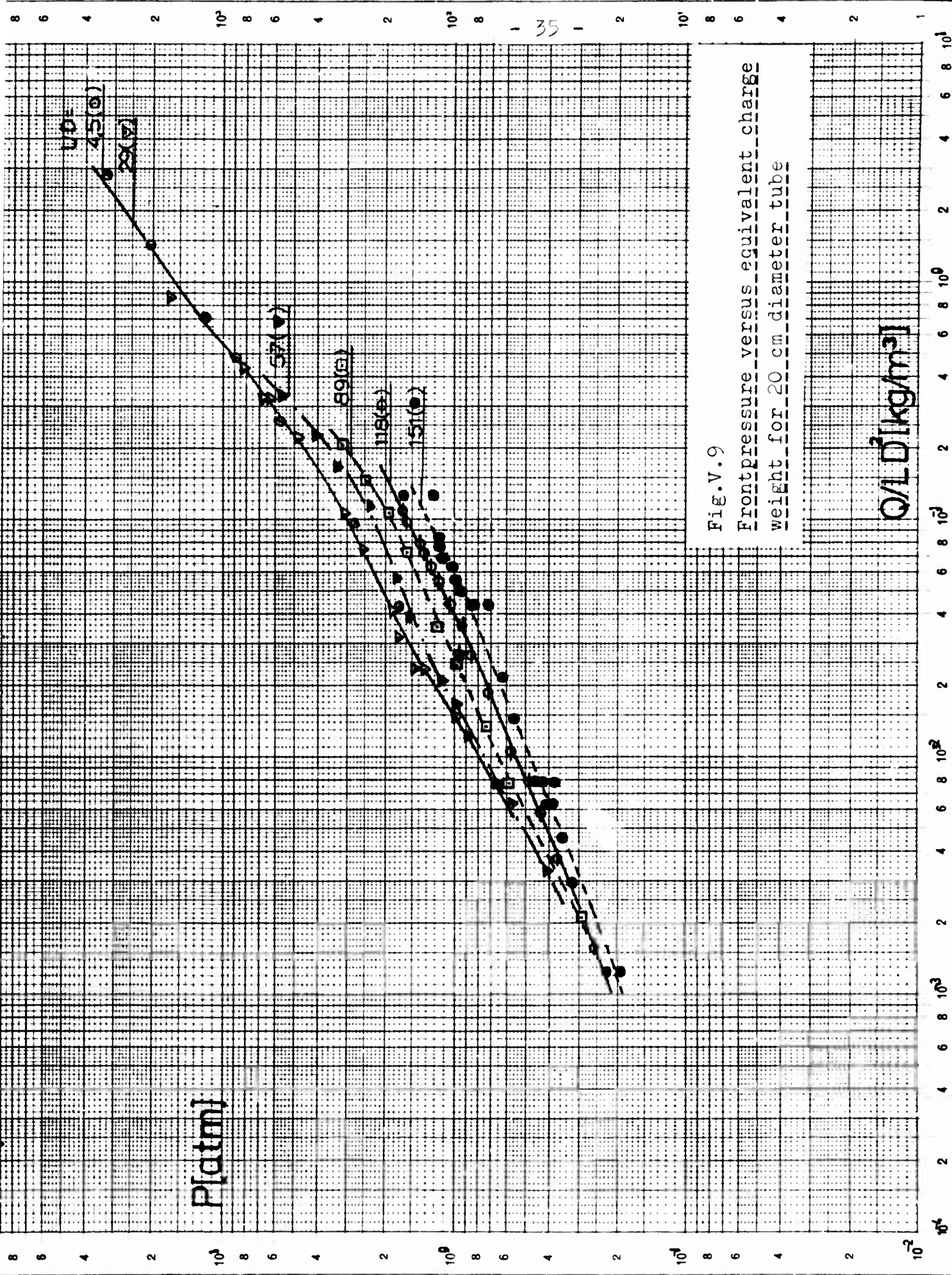
Fig V.8
Front pressure versus
equivalent charge weight
for 5 cm diameter tube

P[atm]

$Q/LD^2 [kg/m^3]$

Fig.V.9

Front pressure versus equivalent charge weight for 20 cm diameter tube



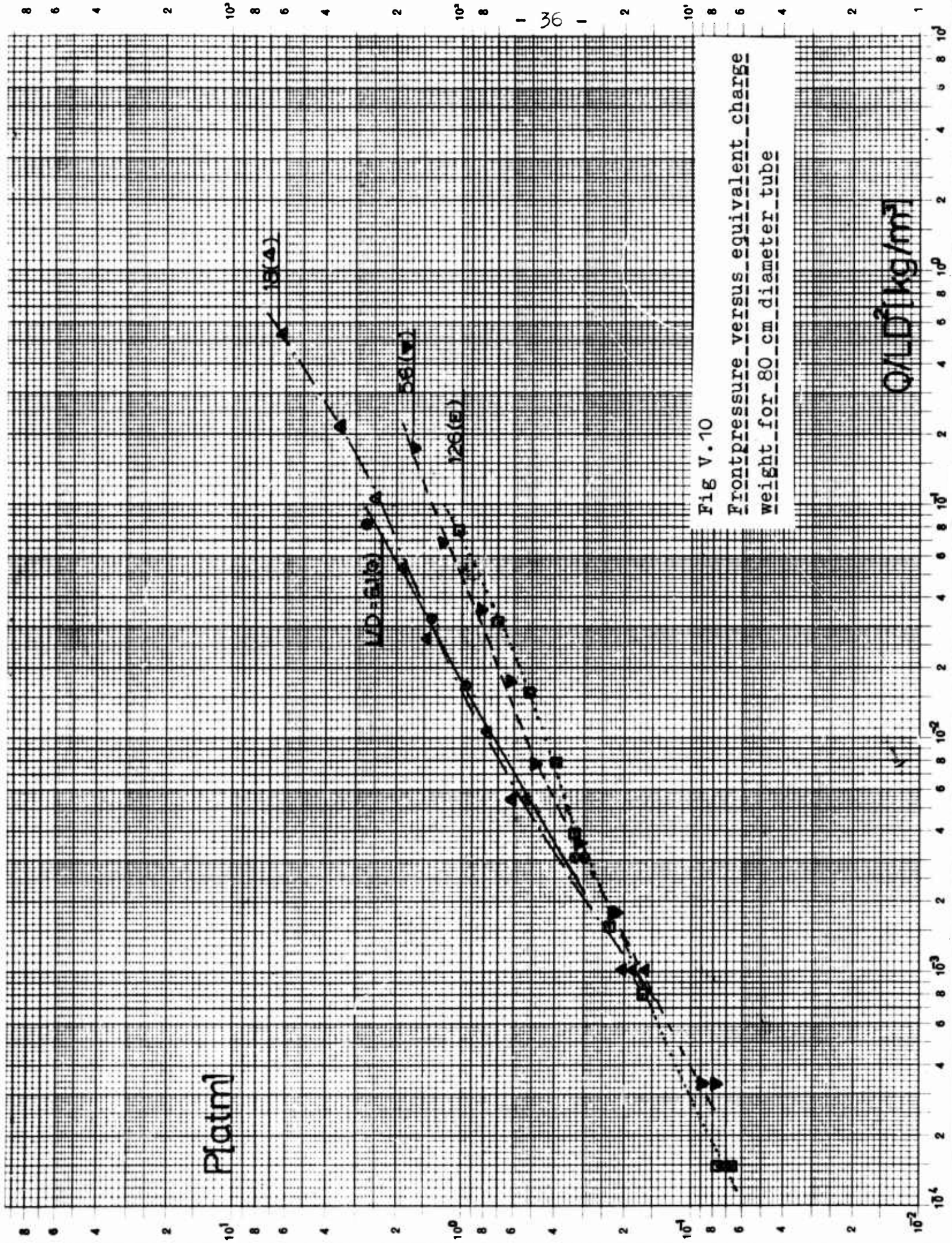


Fig V.10

Front pressure versus equivalent charge weight for 80 cm diameter tube

Q/LD^2 [kg/m²]

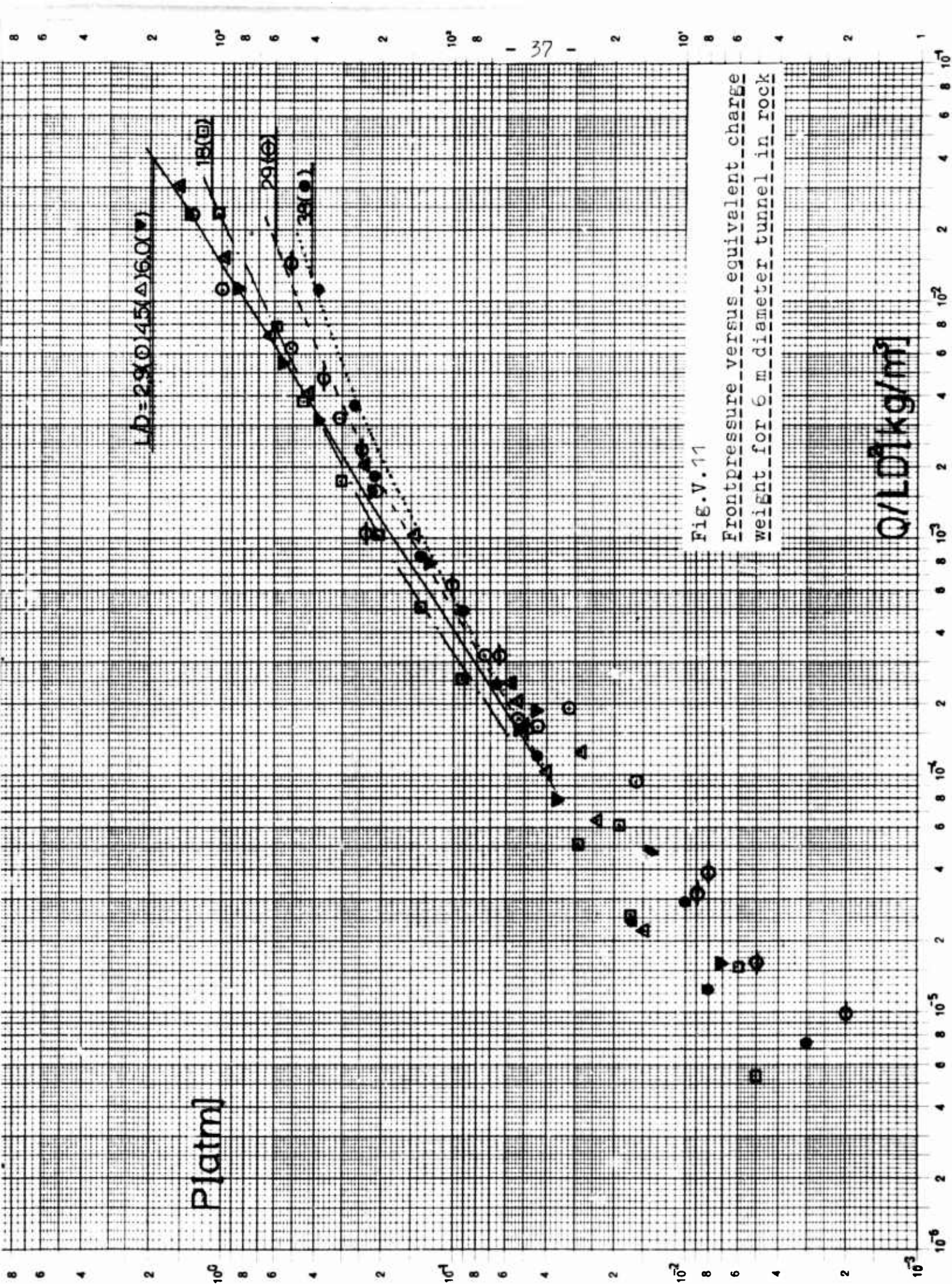
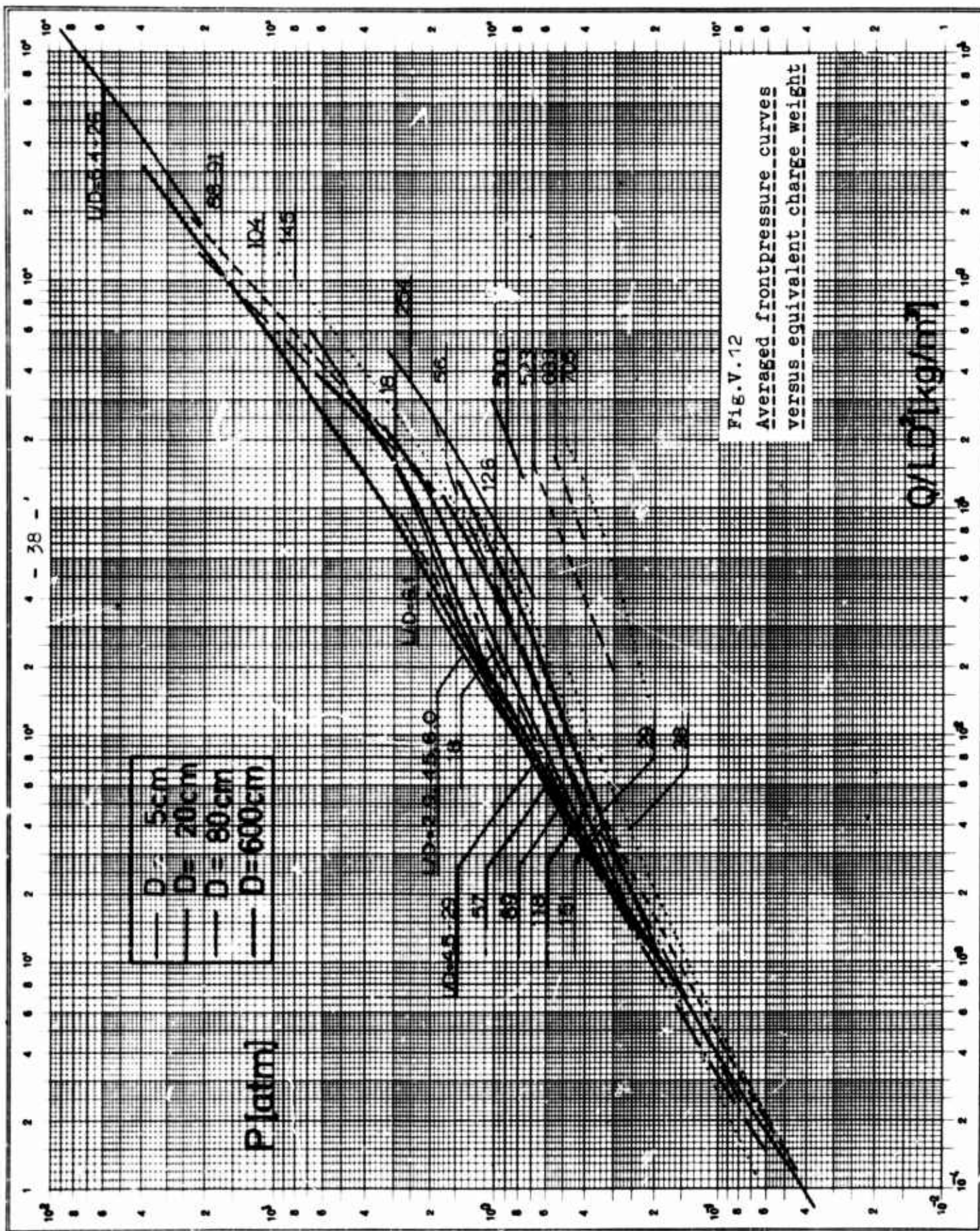


Fig. V.11

Front pressure versus equivalent charge weight for 6 m diameter tunnel in rock



The overall feature is that the deviation from the ideally expected scaled smooth frontpressure curve is greater, the smaller the tube cross section.

Plotting the pressure versus L/D with Q_E as parameter we may extrapolate to $L/D \rightarrow 0$ and get the "unattenuated" scaled pressure curve, $p_{so}(Q_E)$.

The average L/D influence on the attenuation is evaluated to have exponential behaviour as

$$(V.6) \quad p = p_{so} \exp(-k \cdot (L/D))$$

The damping constant k depends on p_{so} and tube/tunnel and is expressed as the fractional loss in frontpressure per diameter of travel, i.e., as

$$(V.7) \quad -D(dp/dx)/p = k$$

This constant is estimated in fig V.13.

The tunnel shows considerably greater wall attenuation than the smoother tubes.

Emerich et al. in ref /4/ gives a value

$k = (1,4 \pm 0,8) \cdot 10^{-3}$ as a mean value, for a 3,5 and 15,3 cm diameter tube with p_{so} between 0,1 and 1 atm, which roughly lies in the region of our estimations.

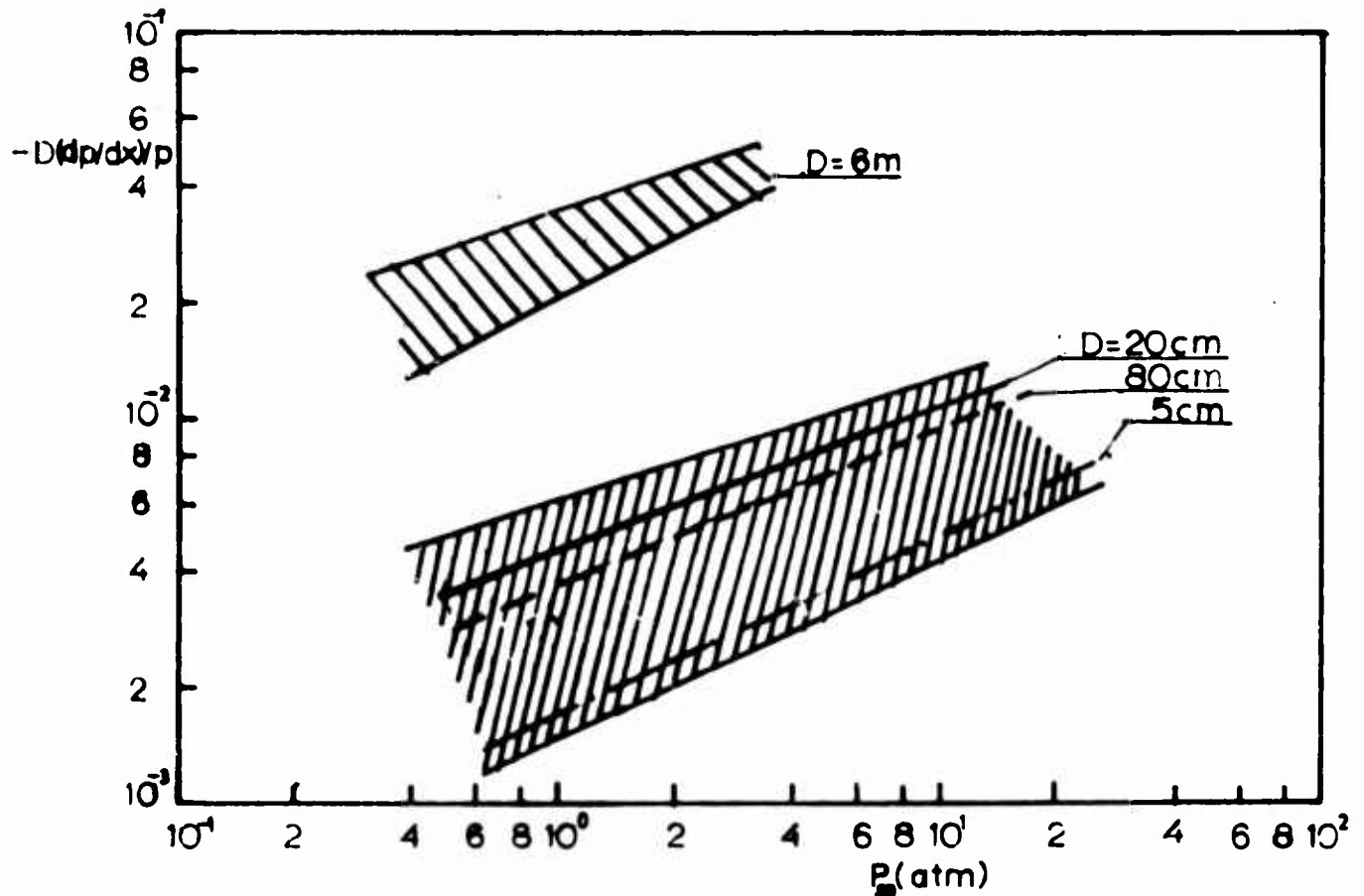


Fig V.13 Fractional changes in pressure from scaled unattenuated curve per unit distance of travel in tube diameters

Comparative tests done by Norwegian Defence Research Establishment /5/ in a tunnel in rock of effective diameter $4,8 \pm 0,5$ m, i.e. roughness about 13% with charges ranging from 10 to 500 kg TNT and $L/D = 1,9 - 12$, shows good agreement with our experiments.

V.2 Impulse

The scaling law proposed in chapter II.2 eq. (II.10) for the impulse I

$$(II.10) \quad \frac{I \cdot D^2}{Q} = g\left(\frac{Q}{LD^2}\right) = g(Q_E)$$

$\left(\frac{I \cdot D^2}{Q}\right)$ hereafter called reduced impulse)

is checked with experiments in fig V.14 - V.18. The data here are considerably fewer than for the pressure which is because rarefaction waves from the open end of the tubes sometimes destroyed the correct pressure time history.

Direct comparison at comparable distances in L/D units in fig V.17 and V.18 shows a significant lower reduced impulse for the tunnel in rock at large L/D (≈ 38) compared with the tubes.

We may use the same procedure as described in V.1 for the pressure letting $L/D \rightarrow 0$ and find the "unattenuated" scaled impulse curve. For $L/D \lesssim 7$ the attenuation is not significantly different for the tubes and tunnel in rock.

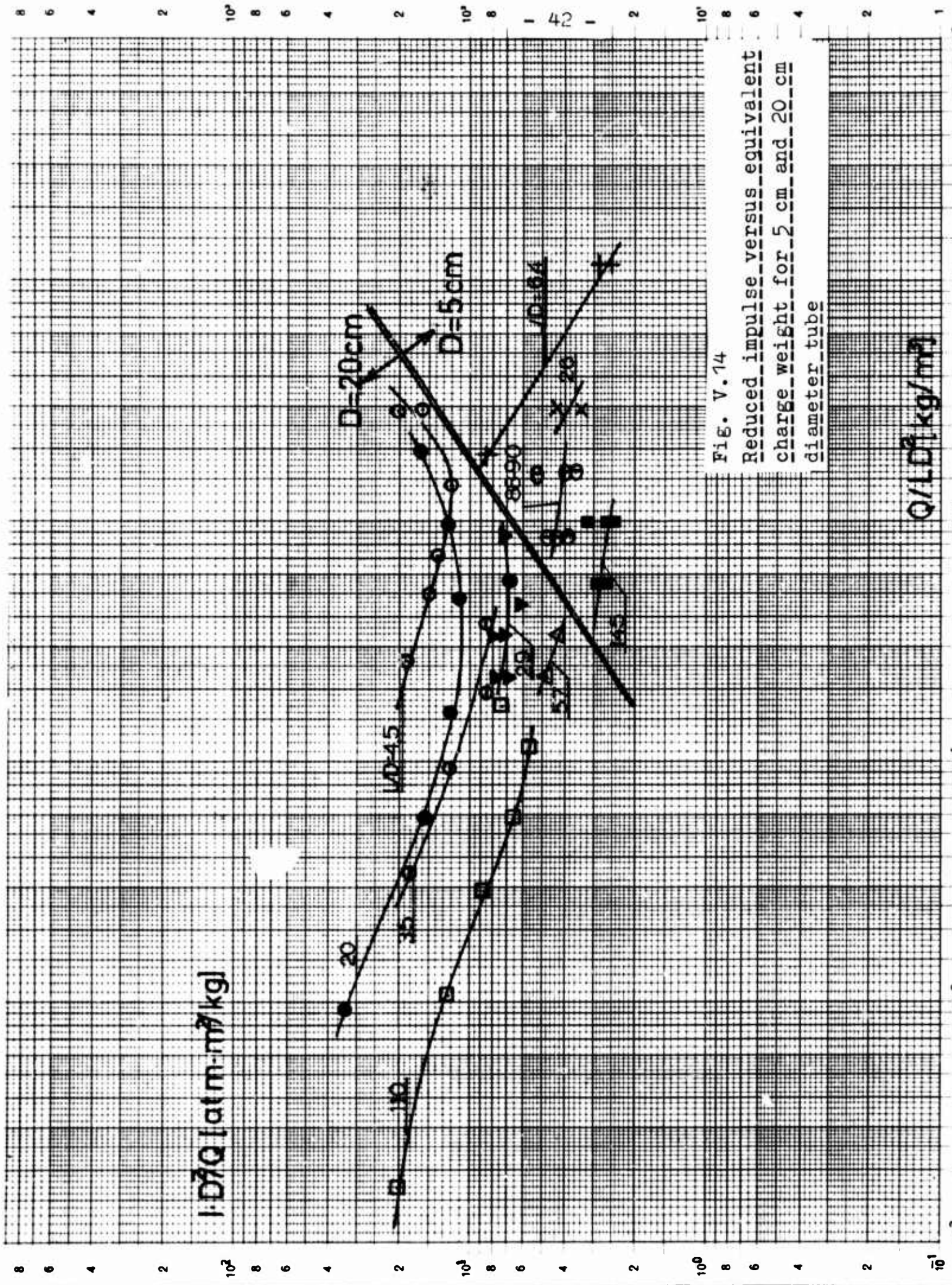


Fig. V.14

Reduced impulse versus equivalent charge weight for 5 cm and 20 cm diameter tube

1-D70 [atm.ms.m³/kg]

2000 2001 2002 2003 2004 2005 2006 2007 2008 2009 2010 2011 2012 2013 2014 2015 2016 2017 2018 2019 2020 2021 2022 2023 2024 2025 2026 2027 2028 2029 2030 2031 2032 2033 2034 2035 2036 2037 2038 2039 2040 2041 2042 2043 2044 2045 2046 2047 2048 2049 2050 2051 2052 2053 2054 2055 2056 2057 2058 2059 2060 2061 2062 2063 2064 2065 2066 2067 2068 2069 2070 2071 2072 2073 2074 2075 2076 2077 2078 2079 2080 2081 2082 2083 2084 2085 2086 2087 2088 2089 2090 2091 2092 2093 2094 2095 2096 2097 2098 2099 2100 2101 2102 2103 2104 2105 2106 2107 2108 2109 2110 2111 2112 2113 2114 2115 2116 2117 2118 2119 2120 2121 2122 2123 2124 2125 2126 2127 2128 2129 2130 2131 2132 2133 2134 2135 2136 2137 2138 2139 2140 2141 2142 2143 2144 2145 2146 2147 2148 2149 2150 2151 2152 2153 2154 2155 2156 2157 2158 2159 2160 2161 2162 2163 2164 2165 2166 2167 2168 2169 2170 2171 2172 2173 2174 2175 2176 2177 2178 2179 2180 2181 2182 2183 2184 2185 2186 2187 2188 2189 2190 2191 2192 2193 2194 2195 2196 2197 2198 2199 2200 2201 2202 2203 2204 2205 2206 2207 2208 2209 2210 2211 2212 2213 2214 2215 2216 2217 2218 2219 2220 2221 2222 2223 2224 2225 2226 2227 2228 2229 2230 2231 2232 2233 2234 2235 2236 2237 2238 2239 2240 2241 2242 2243 2244 2245 2246 2247 2248 2249 2250 2251 2252 2253 2254 2255 2256 2257 2258 2259 2260 2261 2262 2263 2264 2265 2266 2267 2268 2269 2270 2271 2272 2273 2274 2275 2276 2277 2278 2279 2280 2281 2282 2283 2284 2285 2286 2287 2288 2289 2290 2291 2292 2293 2294 2295 2296 2297 2298 2299 2300 2301 2302 2303 2304 2305 2306 2307 2308 2309 2310 2311 2312 2313 2314 2315 2316 2317 2318 2319 2320 2321 2322 2323 2324 2325 2326 2327 2328 2329 2330 2331 2332 2333 2334 2335 2336 2337 2338 2339 2340 2341 2342 2343 2344 2345 2346 2347 2348 2349 2350 2351 2352 2353 2354 2355 2356 2357 2358 2359 2360 2361 2362 2363 2364 2365 2366 2367 2368 2369 2370 2371 2372 2373 2374 2375 2376 2377 2378 2379 2380 2381 2382 2383 2384 2385 2386 2387 2388 2389 2390 2391 2392 2393 2394 2395 2396 2397 2398 2399 2400 2401 2402 2403 2404 2405 2406 2407 2408 2409 2410 2411 2412 2413 2414 2415 2416 2417 2418 2419 2420 2421 2422 2423 2424 2425 2426 2427 2428 2429 2430 2431 2432 2433 2434 2435 2436 2437 2438 2439 2440 2441 2442 2443 2444 2445 2446 2447 2448 2449 2450 2451 2452 2453 2454 2455 2456 2457 2458 2459 2460 2461 2462 2463 2464 2465 2466 2467 2468 2469 2470 2471 2472 2473 2474 2475 2476 2477 2478 2479 2480 2481 2482 2483 2484 2485 2486 2487 2488 2489 2490 2491 2492 2493 2494 2495 2496 2497 2498 2499 2500 2501 2502 2503 2504 2505 2506 2507 2508 2509 2510 2511 2512 2513 2514 2515 2516 2517 2518 2519 2520 2521 2522 2523 2524 2525 2526 2527 2528 2529 2530 2531 2532 2533 2534 2535 2536 2537 2538 2539 2540 2541 2542 2543 2544 2545 2546 2547 2548 2549 2550 2551 2552 2553 2554 2555 2556 2557 2558 2559 2560 2561 2562 2563 2564 2565 2566 2567 2568 2569 2570 2571 2572 2573 2574 2575 2576 2577 2578 2579 2580 2581 2582 2583 2584 2585 2586 2587 2588 2589 2590 2591 2592 2593 2594 2595 2596 2597 2598 2599 2600 2601 2602 2603 2604 2605 2606 2607 2608 2609 2610 2611 2612 2613 2614 2615 2616 2617 2618 2619 2620 2621 2622 2623 2624 2625 2626 2627 2628 2629 2630 2631 2632 2633 2634 2635 2636 2637 2638 2639 2640 2641 2642 2643 2644 2645 2646 2647 2648 2649 2650 2651 2652 2653 2654 2655 2656 2657 2658 2659 2660 2661 2662 2663 2664 2665 2666 2667 2668 2669 2670 2671 2672 2673 2674 2675 2676 2677 2678 2679 2680 2681 2682 2683 2684 2685 2686 2687 2688 2689 2690 2691 2692 2693 2694 2695 2696 2697 2698 2699 2700 2701 2702 2703 2704 2705 2706 2707 2708 2709 2710 2711 2712 2713 2714 2715 2716 2717 2718 2719 2720 2721 2722 2723 2724 2725 2726 2727 2728 2729 2730 2731 2732 2733 2734 2735 2736 2737 2738 2739 2740 2741 2742 2743 2744 2745 2746 2747 2748 2749 2750 2751 2752 2753 2754 2755 2756 2757 2758 2759 2760 2761 2762 2763 2764 2765 2766 2767 2768 2769 2770 2771 2772 2773 2774 2775 2776 2777 2778 2779 2780 2781 2782 2783 2784 2785 2786 2787 2788 2789 2790 2791 2792 2793 2794 2795 2796 2797 2798 2799 2800 2801 2802 2803 2804 2805 2806 2807 2808 2809 2810 2811 2812 2813 2814 2815 2816 2817 2818

18



Fig. V.15.

Reduced impulse versus equivalent charge weight for 80 cm diameter t

 $Q/L: D^2 \text{ kg/m}^2$

$D=6m$

$1 \cdot D^3 Q$ [atm.ms.m³/kg]

$(D=29(\circ) 4,5(\Delta))$

18

38

Fig. V.16.

Reduced impulse versus equivalent charge weight for 6 m diameter tunnel in rock

Q/L [kg/m³]

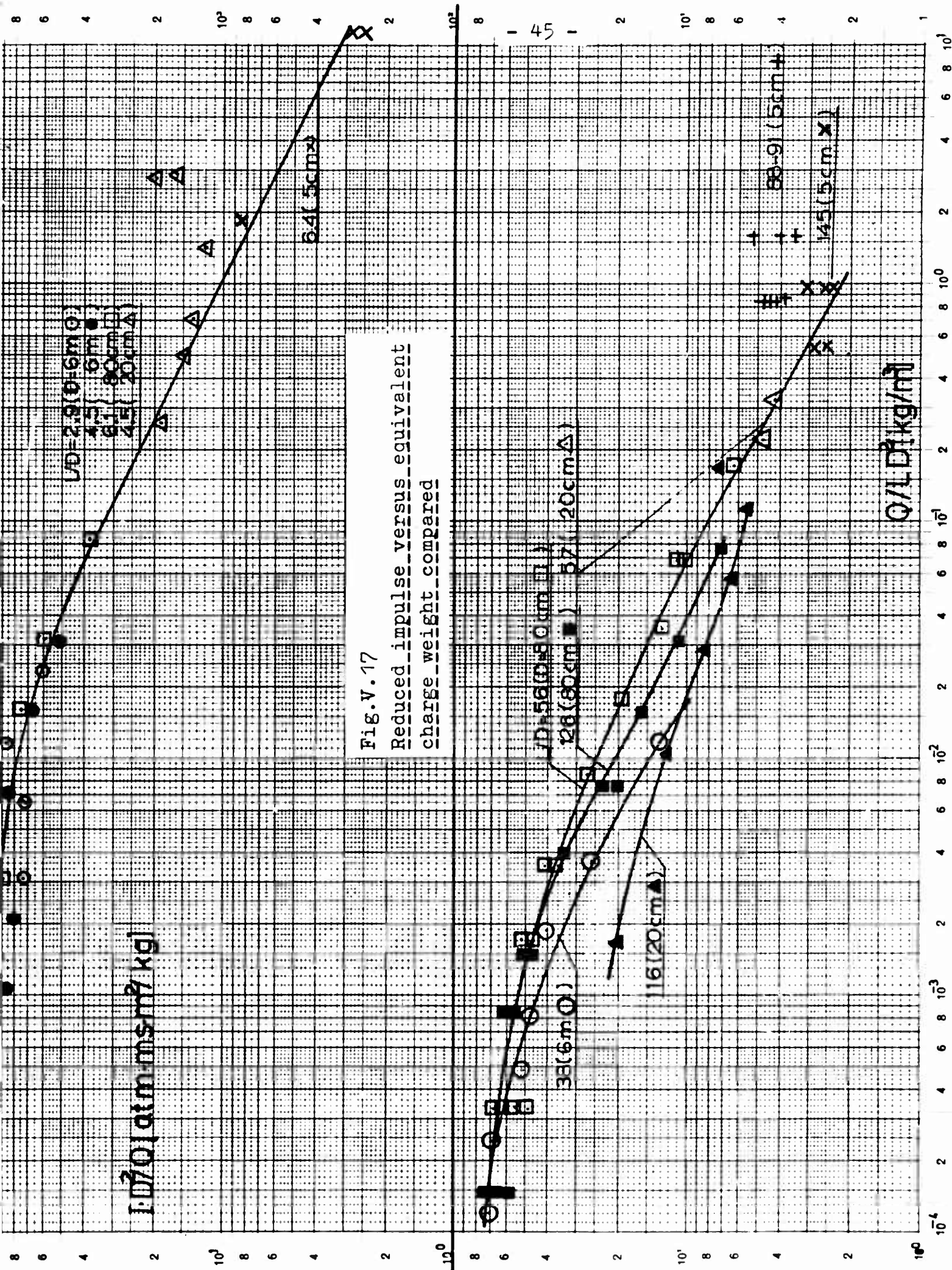


Fig.V.17
Reduced impulse versus equivalent
charge weight compared

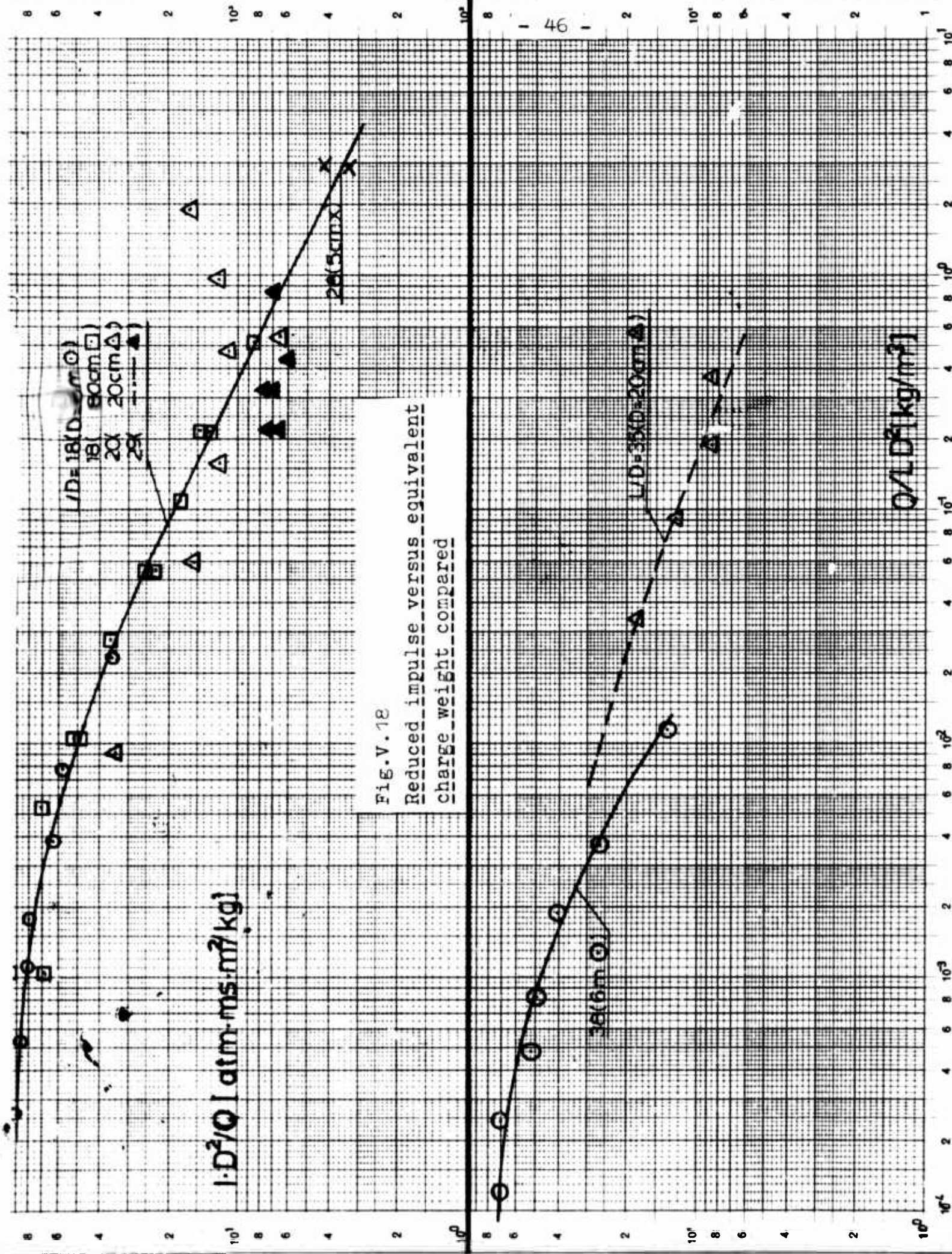


Fig.V.18
Reduced impulse versus equivalent
charge weight compared

V.3 Positive duration

The scaling law proposed in chapter II.2 eq (II.11) for the positive duration t_+

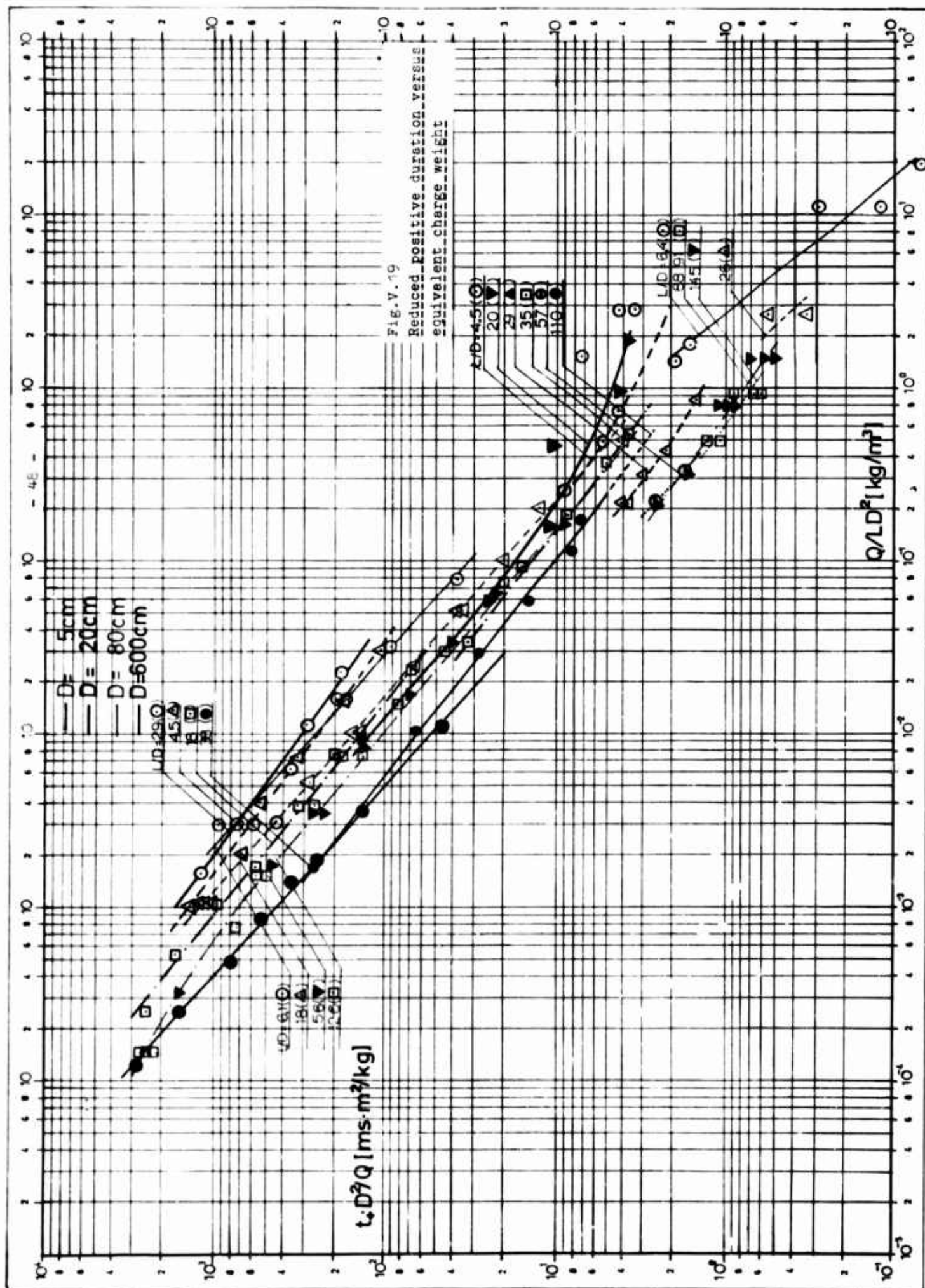
$$(II.11) \quad \frac{t_+ \cdot D^2}{Q} = h\left(\frac{Q}{LD^2}\right) = h(Q_E)$$

is checked with experiments in fig V.19.

We are seeing the same tendency here as for the impulse - lowering of the reduced positive duration curves with increasing L/D values. The wall roughness seems not to have a simple scaled influence.

For $L/D \lesssim 7$ the positive duration seems to scale roughly for all tubes and tunnel.

We may propose here too that loading analysis be made utilizing the $L/D \lesssim 7$ data only to have a safety factor.



V.4 Time of arrival

Time from detonation to blast wave reaches distance L, was found to scale as

$$(II.12) \quad \frac{t_a \cdot D^2}{Q} = i \left(\frac{Q}{LD^2} \right) = i (Q_E)$$

which is checked with the experiments in fig V.20 for all tubes and tunnel in rock. We have no significant deviation in this case from one smooth curve with increased L/D values within the experimental uncertainty

$$\text{For } 10^{-5} \lesssim \frac{t_a D^2}{Q} \lesssim 10^{-2} \left[\frac{\text{ms} \cdot \text{m}^2}{\text{kg}} \right]$$

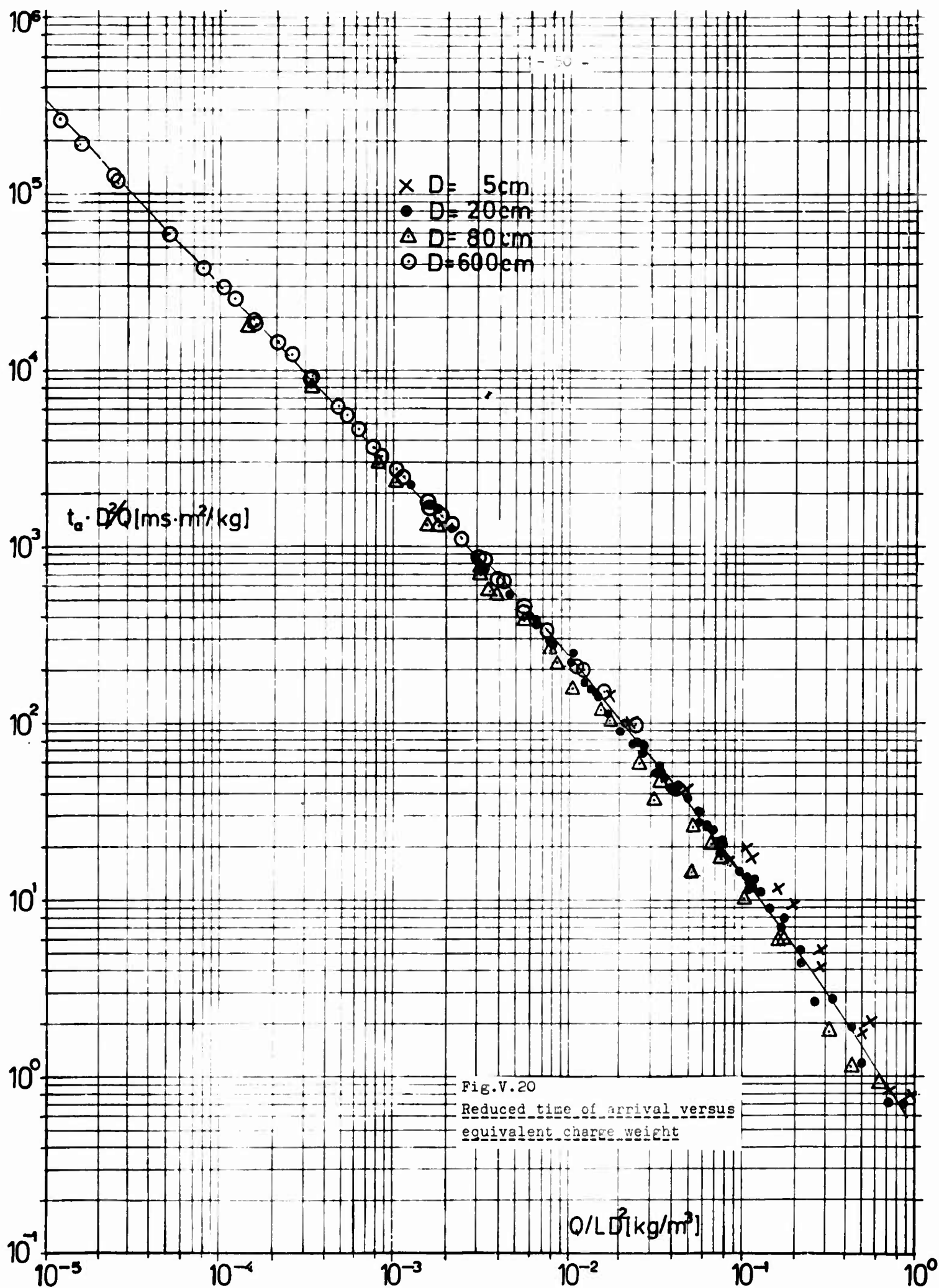
$$\text{and } 10^{-5} \lesssim \frac{Q}{LD^2} \lesssim 10^{-2} \left[\frac{\text{kg}}{\text{m}^3} \right]$$

the scaled curve may roughly be described by the straight line in the log-log plot as:

$$(V.8) \quad \frac{t_a \cdot D^2}{Q} \simeq 2,05 \left(\frac{Q}{LD^2} \right)^{-1,05}$$

or

$$(V.9) \quad t_a (\text{ms}) \simeq 2,05 \frac{D^{0,1} \cdot L^{1,05}}{Q^{0,05}}$$



VI SUMMARY

Frontpressure of an one-dimensional blast wave generated by a charge detonating in a tunnel scales as

$$(VI.1) \quad p = f \left(\frac{Q}{LD^2} \right)$$

with an attenuation dependent on wall roughness and L/D parameter. The average L/D influence on the "attenuation" from an "unattenuated" scaled pressure curve, $P_{so}(Q_E)$ ($L/D \rightarrow 0$), is evaluated to be

$$(V.2) \quad P = P_{so} \exp [-k(L/D)]$$

Estimates of k is given in fig V.13 for different tubes and tunnel in rock.

Typical for $p_{so} \approx 1$ atm, 5, 20 and 80 cm tubes with wall roughness 0,03 - 0,5% have

$$k \approx (4 \pm 2) \cdot 10^{-3}.$$

For the 6 m diameter tunnel in rock, roughness $\approx 8\%$, $k \approx (3 \pm 1) \cdot 10^{-2}$.

The reduced impulse scales as

$$(VI.3) \quad \frac{I \cdot D^2}{Q} = g \left(\frac{Q}{LD^2} \right)$$

with an L/D influence dependent on roughness similar to frontpressure.

The reduced positive duration scales as

$$(VI.4) \quad \frac{t_+ \cdot D^2}{Q} = h \left(\frac{Q}{LD^2} \right)$$

with similar effects as described above.

The reduced time of arrival scales as

$$(VI.5) \quad \frac{t_a \cdot D^2}{Q} = 1 \left(\frac{Q}{LD^2} \right)$$

which does not seem to have a significant L/D dependence

$$\text{For } 10^{-5} \leq \frac{Q}{LD^2} \leq 10^{-2}$$

$$t_a (\text{ms}) \approx 2,05 \frac{D^{0,1} \cdot L^{1,05}}{Q^{0,05}}$$

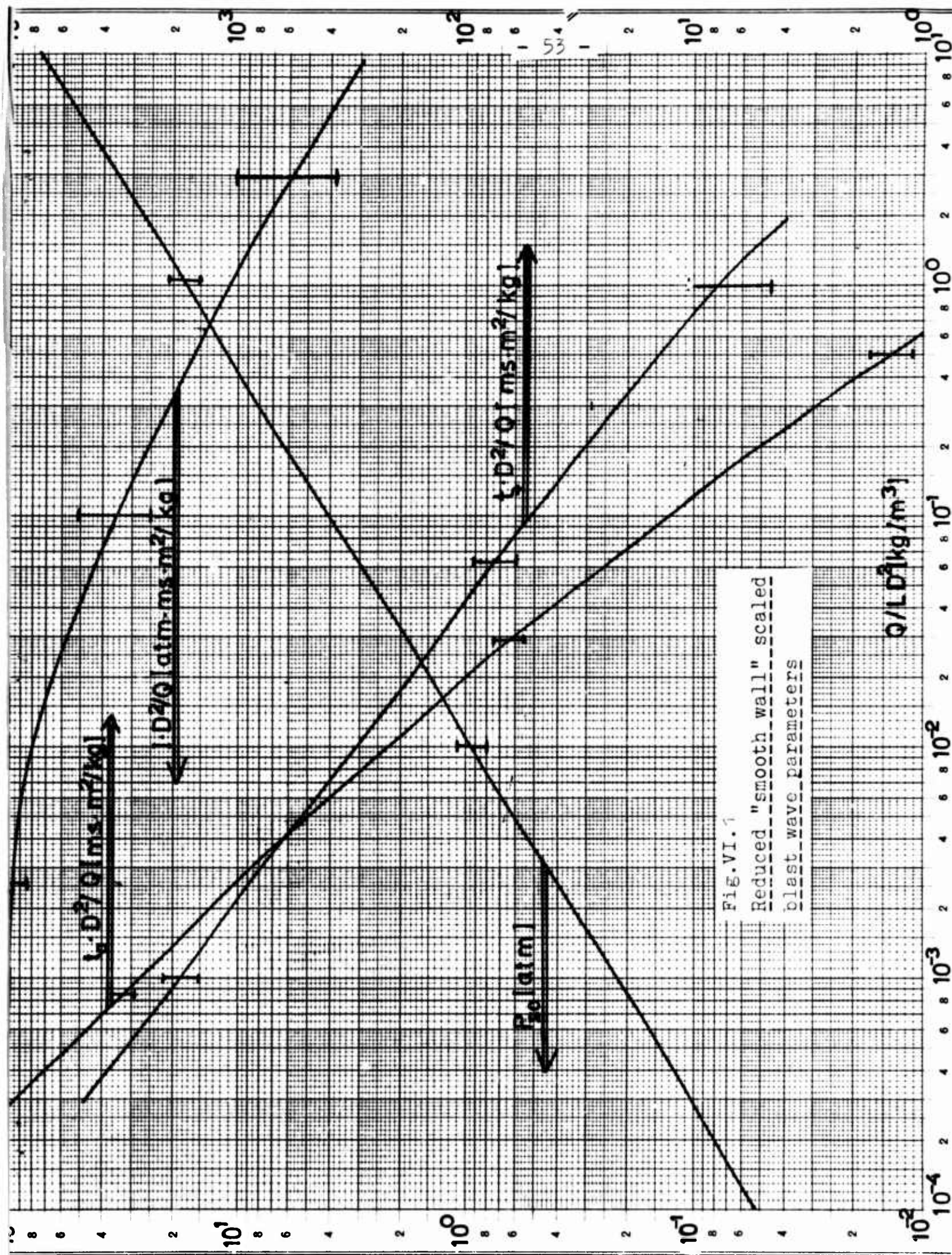
with D(m)

L(m)

Q(kg TNT)

It is recommended that loading analysis to be made utilizing the "smooth tube" or $\lim L/D \rightarrow 0$ data only. It is felt that, although roughness does not seem to scale, any roughness in a tunnel would tend to be a safety factor if doors, equipment etc are designed to withstand "smooth wall" loads.

The "smooth wall" reduced parameters for the blast wave are presented in fig VI.1 with rough estimates of the uncertainty.



REFERENCES

- /1/ Langhaar, H.L.
"Dimensional Analysis and Theory of Models".
John Wiley & Sons, Inc (1951)

- /2/ Cole, R.H.
"Underwater explosions"
Dover Publications, Inc.

- /3/ Eriksson, S.
"Fronttryck ock impuls hos endimensionell stötvåg
vid detonation i tunnel."
(Front pressure and impuls of an one-dimensional
shock wave generated by a charge detonation in
a tunnel).
Report no 103.35 Royal Swedish Administration of
Fortification. (1964).

- /4/ Emerich, R.J. and Curtis, C.W.
"Attenuation in shock tube".
Journal of Applied Physics 24, 360 (1953).

- /5/ Curran, D.R.
"Underground storage of ammunition.
Experiments concerning accidental detonation in
an underground chamber."
Internal report no X-III.
Norwegian Defence Research Establishment (1966).

- /6/ Jenssen, A. - Michalsen, H and Sølberg, A.
"Sikkerhetsspørsmål ved ammunisjonslagre."
Fortifikatorisk notat nr 26/65.
Norwegian Defence Construction Service (1965).